



5-2009

Numerical simulation (a lumped transient model) for QPS modular coils with embedded copper tubes and subsequent experimental verification

Bhargav Telikicherla Kandala
University of Tennessee

Follow this and additional works at: https://trace.tennessee.edu/utk_gradthes

Recommended Citation

Kandala, Bhargav Telikicherla, "Numerical simulation (a lumped transient model) for QPS modular coils with embedded copper tubes and subsequent experimental verification. " Master's Thesis, University of Tennessee, 2009.
https://trace.tennessee.edu/utk_gradthes/5733

This Thesis is brought to you for free and open access by the Graduate School at TRACE: Tennessee Research and Creative Exchange. It has been accepted for inclusion in Masters Theses by an authorized administrator of TRACE: Tennessee Research and Creative Exchange. For more information, please contact trace@utk.edu.

To the Graduate Council:

I am submitting herewith a thesis written by Bhargav Telikicherla Kandala entitled "Numerical simulation (a lumped transient model) for QPS modular coils with embedded copper tubes and subsequent experimental verification." I have examined the final electronic copy of this thesis for form and content and recommend that it be accepted in partial fulfillment of the requirements for the degree of Master of Science, with a major in Mechanical Engineering.

Madhu S. Madhukar, Major Professor

We have read this thesis and recommend its acceptance:

Accepted for the Council:

Carolyn R. Hodges

Vice Provost and Dean of the Graduate School

(Original signatures are on file with official student records.)

To the Graduate Council:

I am submitting herewith a thesis written by Bhargav Telikicherla Kandala entitled "Numerical Simulation (A Lumped Transient Model) for QPS Modular Coils with embedded Copper Tubes and subsequent Experimental verification". I have examined the final electronic copy of this thesis for form and content and recommend that it be accepted in partial fulfillment of the requirements for the degree of Master of Science, with a major in Mechanical Engineering.

Madhu S. Madhukar

Major Professor

We have read this thesis and
recommend its acceptance:

Cheng-Xian (Charlie) Lin

Thomas E. Shannon

Accepted for the Council:

Carolyn R. Hodges

Vice Provost and Dean of the
Graduate School

(Original signatures are on file with official student records.)

**Numerical Simulation (A Lumped Transient Model) for QPS Modular Coils with embedded Copper
Tubes and subsequent Experimental verification**

**A Thesis Presented for the
Master of Science
Degree
The University of Tennessee, Knoxville**

Bhargav Telikicherla Kandala

May 2009

DEDICATION

This thesis is dedicated to my parents Mr. T.K.Gopala Krishna and Mrs. T.K.Mani, to my brother T.K.Sampath who made it possible for me to come and pursue my studies here in United States and to my guide & mentor Dr. Madhu S. Madhukar.

ACKNOWLEDGMENTS

Grad school has come and gone in the blink of an eye. There are many who have facilitated through my graduation. I hold enormous gratitude to Dr. Madhu S. Madhukar for giving me this excellent opportunity to work for the QPS project and interact with ORNL researchers. He, being a constant motivator, supporter and my guide on this project has led to the current results yielded. It was always a learning process with him and as he quotes “Our discussions are never like a teacher and a student but you teach me in the same manner of how I did”, which has built a great rapport. I am lucky to have worked as his research assistant because his guidance was just not constrained to research. He provided me with unlimited direction and ideas during my work on this project and taught me so much about Numerical Simulation, designing experiments in the lab, and just being an engineer. He mentored my focus in critical situations for which I owe him a lot. He spent much time reviewing my work and editing my reports and thesis chapters amidst his tight schedule. It was a crucial period in building my career and this thesis is a result of his effort and belief in me.

I am highly indebted to the Magnet Development Laboratory for their continued financial support throughout the length of my study. I would like to thank Dr. Paul Groanson and Mr. Kevin Freudenberg for giving their expertise during our experimental design and special thanks to Dr. Paul Groanson for helping me with the theoretical concepts used in the numerical simulation. I would like to thank Dr. Tom Shannon for his constant encouragement in our weekly meeting. Special Thanks to Mr. Joe and Mr. Jim for helping us with fixing the conductor in our experimental design. Overall, it was a marvelous learning experience working with the QPS team with their valuable input.

I would like to thank Dr. Cheng-Xian (Charlie) Lin and Dr. Tom Shannon for serving in my committee. Also, I would like to thank Mr. Julius Gunn for helping with the experimental setup and designing the conductor model in Inventor©.

It's particularly important to thank my parents Gopala Krishna and Mani, my brother Sampath and this list would never end without expressing my heartfelt thanks to all my beloved friends here in United States and India.

ABSTRACT

The Quasi-Poloidal Stellarator (QPS) consists of complex shaped modular coils consisting of a tightly packed Cu-polymer composite to carry the high current needed to develop the plasma. During this process, the conductor temperature rises to about 60°C. Before the next current pulse, the conductor must be cooled to room temperature in order to prevent temperature ratcheting over the duty cycle. Computational analysis on various cooling schemes across the conductor cross-section showed that the best results are achieved by internal cooling via copper tubes embedded in the middle of each conductor.

The motivation for this research was to develop a simple engineering tool capable of predicting the cooling response of the centrally cooled long conductors and for this purpose a lumped transient model was developed. In this model, the conductor length was divided into equal number of segments of uniform length. Each water element underwent heat transfer with each composite element as it moved through inlet of tube to outlet. The effect of temperature gradient across the conductor width was modeled by introducing a radial heat resistance length parameter (L^*). To verify the model predictions, a 5.5 m long conductor with embedded copper tube in the middle was cast in a racetrack shape by vacuum impregnating the conductor with CTD 403 cyanate ester polymer. The conductor was then heated to two different temperatures ($\Delta T = 60^\circ\text{C}$ & 80°C) and then cooled by water flowing through the tube at different flow rates. The exit water temperature and the outer surface temperature of the conductor at various points across its length were monitored during the entire experiment. One of the experimental data sets was used to obtain the value of L^* and the same L^* was used to predict the cooling curves for all other ΔT and flow rate combinations. The comparison between experiments and model predictions show that the transient lumped analysis in conjunction with the radial heat resistance parameter provided a good engineering tool to understand the cooling behavior of long conductors. The model was then applied to the actual QPS conductor (36 m long) and its cooling curves were predicted.

TABLE OF CONTENTS

INTRODUCTION.....	1
LITERATURE REVIEW.....	5
EXPERIMENTATION.....	9
3.1. Details of Experimental Facility.....	9
3.2. Experimental Design.....	13
3.3. Experimental Procedure.....	19
4. NUMERICAL SIMULATION.....	21
4.1. Elemental Approach / Lumped Transient Model.....	21
4.2. Biot Number Calculation.....	27
4.3. Introduction of Heat resistance parameter.....	29
5. RESULTS AND DISCUSSIONS.....	30
5.1. Comparison between Experimental and Lumped Transient Model Results.....	30
6. CONCLUSIONS.....	53
6.1 Experimental procedure for heating and cooling of 5.5m (~18ft) QPS conductor.....	53
6.2 Heat transfer analysis of the conductor using the elemental approach.....	54
7. FUTURE WORK.....	55
7.1 Elemental Approach (Lumped Transient Model).....	55
REFERENCES.....	56
APPENDIX A	60
APPENDIX B	67
APPENDIX C.....	74
VITA.....	77

LIST OF TABLES

Table		Page
4.1	Values used in the Lumped Transient Model algorithm	26
5.1	Material properties used in the Lumped Transient Model algorithm	31
5.2	Correlation Coefficient for all the flow rates	47
5.3	Reynolds numbers calculated in the model for different flow rates	49

LIST OF FIGURES

Figure	Page
1.1 Cut-away section of QPS	2
1.2.1 Various cooling concepts analyzed	3
1.2.2 Various cooling concepts analyzed	4
3.1.1 Enlarged view of square cross section of the copper	9
3.1.2 Coil wound on the form for vacuum pressure impregnation	10
3.1.3 Cure cycle used for the conductor as described by CTD 403 manufacturer	11
3.1.4 Test coil after vacuum pressure impregnation	11
3.1.5 Conductor used for Experiments with thermocouples fixed at different locations	12
3.2.1 Temperature Profile of Heat tape heating	14
3.2.2 Final Experimental setup	15
3.2.3 Temperature profile of conductor when heated to 63°C and cooled by water flow rate Of 0.1GPM using the initial experimental setup	16
3.2.4 Temperature profile of conductor when heated to 63°C and cooled by water flow rate Of 0.1GPM using the initial experimental setup monitoring the inlet water temperature	17
3.3.1 Temperature profile of conductor when heated to 63°C and cooled by water flow rate Of 0.1GPM using the final experimental setup	20
4.1.1 Square conductor modeled as a circular conductor	21
4.1.2 Line diagram of the elemental approach	22
4.1.3 Lumped Heat capacity system	23
4.1.4 Line diagram of the movement of elements	25
4.3.1 A typical comparison between the Experimental and Lumped transient model result	28
5.1 Comparisons between experimental and predicted results when conductor is heated to 62°C and cooled by water flow rate of 0.1GPM	32
5.2 Comparisons between experimental and predicted results when conductor is heated to 61.4°C and cooled by water flow rate of 0.15GPM	33

5.3	Comparisons between experimental and predicted results when conductor is heated to 62.37°C and cooled by water flow rate of 0.2GPM	34
5.4	Comparisons between experimental and predicted results when conductor is heated to 62.76°C and cooled by water flow rate of 0.25GPM	35
5.5	Comparisons between experimental and predicted results when conductor is heated to 61.2°C and cooled by water flow rate of 0.3GPM	36
5.6	Comparisons between experimental and predicted results when conductor is heated to 81.5°C and cooled by water flow rate of 0.1GPM	37
5.7	Comparisons between experimental and predicted results when conductor is heated to 80.2°C and cooled by water flow rate of 0.15GPM	38
5.8	Comparisons between experimental and predicted results when conductor is heated to 80.51°C and cooled by water flow rate of 0.2GPM	39
5.9	Comparisons between experimental and predicted results when conductor is heated to 81.042°C and cooled by water flow rate of 0.25GPM	40
5.10	Comparisons between experimental and predicted results when conductor is heated to 80.54°C and cooled by water flow rate of 0.3GPM	41
5.11	Comparisons between experimental and predicted results for the exit water temperature when conductor is heated to ≈60° and cooled by five different flow rates	42-43
5.12	Comparisons between experimental and predicted results for the exit water temperature when conductor is heated to ≈80° and cooled by five different flow rates	44-45
5.13	Predicted cooling behavior results for 120ft long QPS conductor when heated to 60° and cooled by a water flow rate of 0.1GPM	51
5.14	Predicted cooling behavior results for 120ft long QPS conductor when heated to 60° and cooled by a water flow rate of 0.2GPM	52

1. INTRODUCTION

Depleting petroleum reserves combined with increasing global demand for energy has forced mankind to look for other sources of energy. The global energy consumption is expected to escalate dramatically, increasing by 71% in 2030 and continuing to rise. Energy shortages would have a dramatic impact on every area of modern life: business, transport, food, health and communications. This looming crisis has drawn scientific minds and encouraged radical research into arcane technologies, such as nuclear fusion technology. The most obvious advantage of the fusion technology is the virtual inexhaustibility of its fuels, which are cheap and widely accessible. The use of fusion power plants could substantially reduce the environmental impacts of increasing world electricity demands since, like nuclear fission power, it would not contribute to acid rain or the greenhouse effect. However, the criticality of technology is that fusion needs inhumanly high and sustainable reaction temperatures. Such temperatures are realized by producing and sustaining Plasma, popularly called the fourth state of matter by using magnetic fields to confine the plasma. The most highly developed system of this type is the tokamak, with the stellarator being next most advanced. A 500-MW heat generating fusion plant using tokamak magnetic confinement geometry is currently being built in France called ITER.

Magnetic confinement fusion attempts to create the conditions needed for fusion energy production by using the electrical conductivity of the plasma to contain it with magnetic fields. Stellarators are a class of magnetic fusion confinement devices used for this purpose. Quasi-Poloidal Stellarator (QPS), Figure 1.1, is one such device under development at Oak Ridge National Lab.

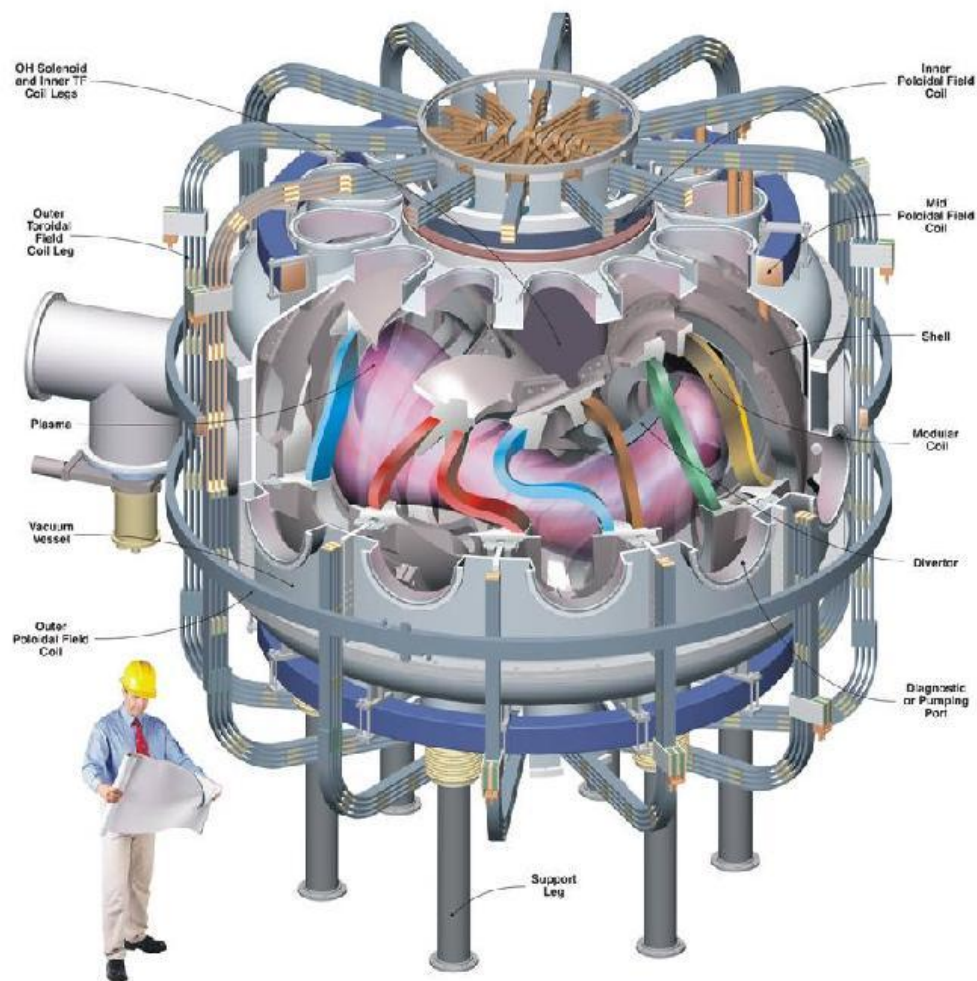


Fig. 1.1: Cut-away section of QPS

QPS is a low aspect ratio, concept exploration experiment with a non-axisymmetric, near poloidally symmetric magnetic configuration [1]. QPS consists of complex shaped modular coils that are made of Copper-CTD 403 cyanate ester composite to carry the high current needed to develop the Plasma. During the operation of the QPS, when high current pulse ($\sim 30,000$ amperes) is passed through the long insulated conductor to produce plasma, its temperature is expected to rise from room temperature (20°C) to about 60°C . Before the next current pulse is passed, the conductor needs to be cooled to room temperature in order to prevent temperature ratcheting over the duty cycle. Based on the numerical analysis of various cross-sectional configurations for cooling the modular coils (Figure 1.2.1), Freudenberg et al. [2] concluded that the most efficient method was embedding the copper tube inside the conductor, Figure 1.2.2. Thermal Modeling and verification of a QPS modular coil, by Anuj [3], also discusses the thermal cooling requirements and need & location for cooling methods.

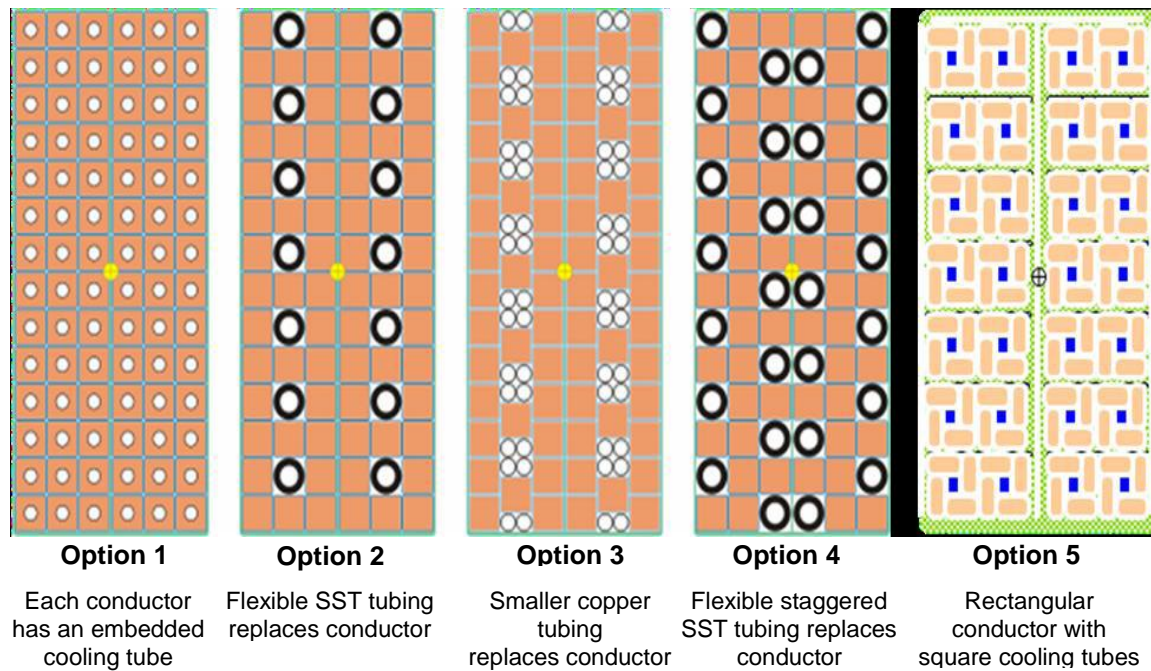


Fig. 1.2.1: Various cooling concepts

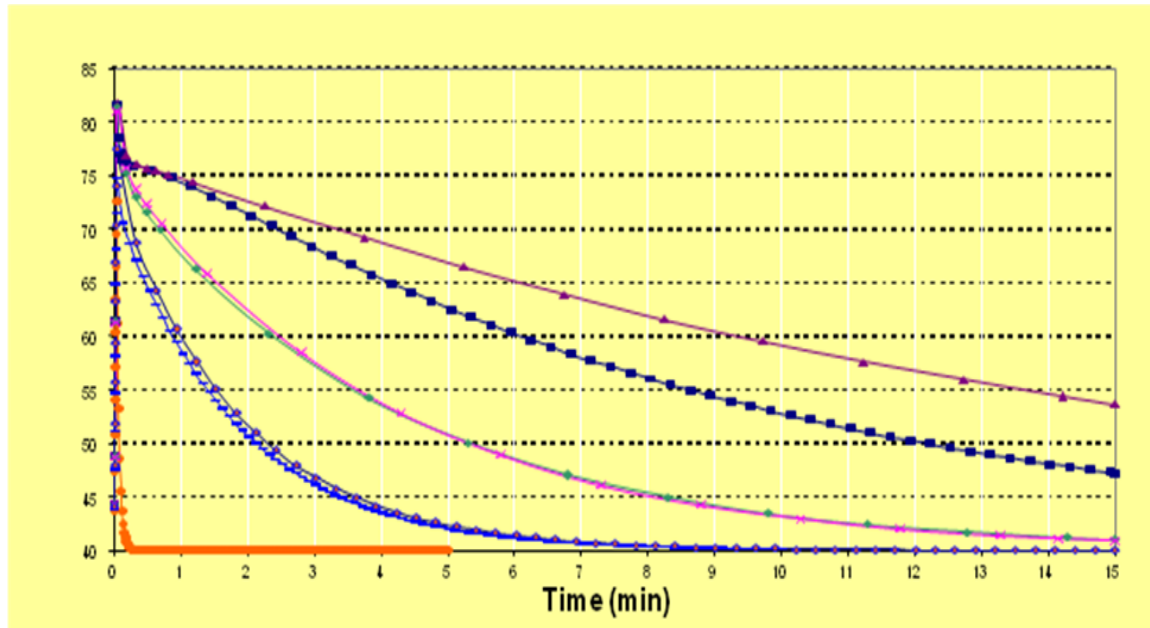


Figure 1.2.2: Temperature–Time curves calculated at the inner most point of the winding pack for different cooling arrangements shown in Fig. 1.2.a. The tube arrangement shown in Option I with copper cooling tubes in the middle of each conductor produces the maximum cooling².

The cooling scenario encountered in internally cooled QPS conductors is a transient state problem. To predict the cooling behavior of these long conductors (~120 ft) using Finite elements requires tremendous computational sources. In this thesis, a semi-empirical numerical approach was developed in MATLAB® software to predict the cooling rate of these conductors. The predictions were compared with the experimental data obtained from a 5.5m (18-ft) long conductor for several combinations of temperature and flow rates. The same model was then used to predict the cooling response of 120-ft long QPS conductor.

2. LITERATURE REVIEW

While there are several studies published on transient heat transfer analysis in composite material research on transient heat transfer in long conductors is scarce. Many researchers have investigated the effect on heat transfer due to different types of flow of fluids and gases and parameters that affect the heat transfer rate. Studies on heat transfer have been conducted using a) multitude of tubes such as horizontal tube with various cross sections and orientations, b) tubes rotating around a parallel axis as used for internal cooling in some electrical machines; c) cooling tubes with different configurations like straight and wavy tubes (waviness along the length of the tube); slabs etc.

Some of the work pertinent to this thesis is presented in the following pages.

C.W. Leung and S. D. Probert [4] studied the forced convective heat transfer properties in a duct with triangular cross section. They obtained the values of Nusselt number experimentally for a range of Reynold's numbers covering the laminar and turbulent phases taking into account the hydraulic diameter. This research concluded that greater rate of heat transfer could be achieved because of the sharp edges of the equilateral-triangle cross-sectioned duct and recommended that it could be used in heat exchanger design practice. C.W. Leung and S. D. Probert [5] also conducted the above study for isosceles cross section of the tube. It was concluded in the study that the maximum heat transfer coefficient could be obtained by having the equilateral triangle cross-section for the same hydraulic diameter. Also higher turbulence and rounding of the corners diminished the inhibition to heat transfer posed by the triangular corners. These research methods [4-5] cannot be applied directly to QPS conductors but the significance of Nusselt number and overall heat transfer coefficient for the heat transfer rate has been taken into account.

G. Wang and S. P. Vanka [6] studied numerically the rates of heat transfer for flow through wavy (sinusoidally curved) passages. Beyond Reynold's number of 180, oscillations in the flow led to the destabilization of the thermal boundary layer. During the transitional flow, the heat and mass transfer

increased to nearly 2.5 times. The main concentration of this research was to study the effects of organized and disorganized fluid flows that contribute to heat transfer when flowed through the top and bottom of corrugations. The fluid flow patterns and its effects are not the major issues for QPS conductors. Yasuo Mori et al., [7] investigated the forced convective heat transfer property in a straight tube rotating along a parallel axis taking into account the secondary flow due to rotation about the axis. They studied the effects of buoyancy force on forced laminar convective heat transfer in a uniformly heated horizontal tube. X. Lu et al., [8] solved a transient multi dimensional heat conduction problem in a composite circular cylinder. Time dependant temperature boundary condition was considered as a Fourier series. A novel approach of applying separation of variables in their multi dimensional case has been presented. X. Lu et al., [9] developed another approach to solve the time dependant multi dimensional composite cylinder slab conduction problem with a time dependant boundary condition. They removed the instability due to the existence of imaginary Eigen values in other numerical schemes by their approach of using Laplace transforms and separation of variables. These research methods [8-9] were novel in their approach without needing any numerical schemes and computational sources, but they cannot be applied for predicting the cooling rate of the QPS conductors because of its unknown boundary conditions. E.K. Kalinin et al., [10] presented an analysis and experimental data on the unsteady heat transfer of gases and liquids flowing in tubes under the conditions of heating/cooling and variation in the flow rate, heat release in the tube walls, and entrance flow temperature. Yuzhi Sun et al., [11] developed a method to solve a transient heat conduction problem in a one-dimensional three-layered composite slab using the Eigen function method. This method was found to reduce the inaccuracies caused by numerical solutions for the same problem especially when one of the slabs has radically different properties or is much narrower than the others. F. de Monte [12] developed an analytic approach which is described to be simpler than the earlier models to solve one dimensional transient conduction problem in a multi layered composite slab. The method analyses the transient response of one dimensional multilayered composite slab to the sudden variations of temperature of the surrounding fluid. The solution is obtained by applying the method of separation of variables to the heat conduction partial differential equation. F.de.Monte [13] extended this approach to transient multi-layer problems. This method is applied to composites of any number of layers, and in particular, it allows for composite media

of rectangular, cylindrical and spherical layers, which are in perfect thermal contact. Abram Dorfman [14] investigated the temperature distribution when a thin film of cold fluid is flowing on a semi-infinite flat plate. Evaporation and sputtering were taken into account. In this study, the finite portion of the plate covered by the film and the dry portion of the plate are studied separately.

These methods were useful in determining the transient temperature profile when the boundary conditions are specified. In the QPS composite coils, only the inlet water temperature and the initial conductor temperature are known. Also, the actual temperature gradient in the radial direction of the very long conductor (~120 ft) is not of much interest. The most important pieces of information needed for the QPS design are the time it takes to cool the conductor to its initial temperature and its dependence on the water flow rate and inlet water temperature. Such information can easily be obtained with reasonable accuracy from the lumped transient analysis.

The Lumped Transient Analysis [15] is used to solve a transient state problem where a solid is considered as one lump and its internal resistance is negligible in comparison with the surface resistance. In this thesis, A numerical model was developed in MATLAB© software using this analysis to predict the cooling behavior of the internally cooled QPS conductors by dividing the conductor length into equal segments where each segment is considered as a lump. The study by P.Goranson et al [16] appears to be the first published work on the application of the lumped analysis to predict the heat transfer characteristics in graphite tiles for plasma facing components (PFC) for the National Compact Stallerator Experiment (NCSX). The results obtained were used to validate thermal analyses predictions obtained with other numerical methods. The first known work on the application of lumped transient analysis to predict the cooling of long tubes is a thesis by Shankar [17]. The only verification of the lumped model was provided by comparing the model predictions with those from the finite element model for a very short (1 inch) conductor length. And even for such a short conductor length, there was qualitative disagreement between the predictions from the two approaches. While transient lumped approach provides a starting point for a relatively simpler heat transfer analysis in long tubes, the Biot numbers used in the analysis were very large and thus in contradiction with the assumptions of the lumped

analysis. The issue of Biot number is discussed in more detail in sections below. In this thesis, the lumped transient model as developed by Shankar [17] is modified by introducing an additional radial heat resistance parameter. Such modification eliminates the Biot number discrepancy as well as produces a good agreement between experiments and predictions.

3. Experimental Setup:

3.1. Details of Experimental Facility:

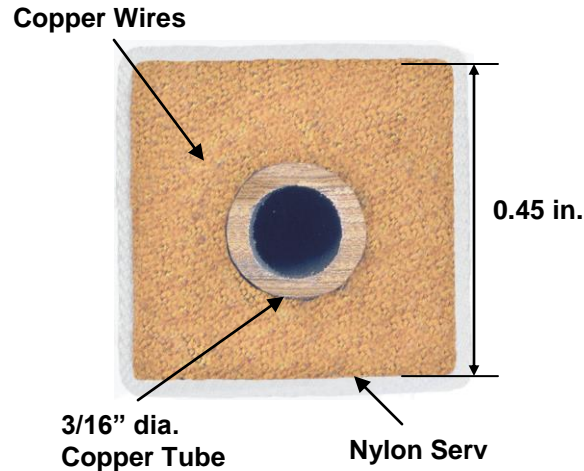


Fig. 3.1.1: Enlarged view of square cross section of the copper

The conductor used in this study was supplied by New England Wire wound on a 3-ft spool. The conductor was a tightly bound, glass cloth wrapped, 0.45 in x 0.45 in cross-section square having copper strands running parallel to the conductor and a 3/16-in diameter copper tube placed in the middle, Figure 3. 1.1

The conductor was hand-laid continuously four turns in a racetrack shaped stainless steel mold such that the cross-section of the racetrack conductor was again a square of approximate dimensions of 0.90 in x 0.90 in. The four continuous turns provided a total conductor length of about 18 ft. The mold consisted of two inlet and two exit ports for polymer impregnation of the conductor. The mold and the conductor assembly were vacuum-sealed by wrapping it with Kapton tape. The assembly was then wrapped with heat tapes, Figure 3.1.2, and covered with insulation blanket.

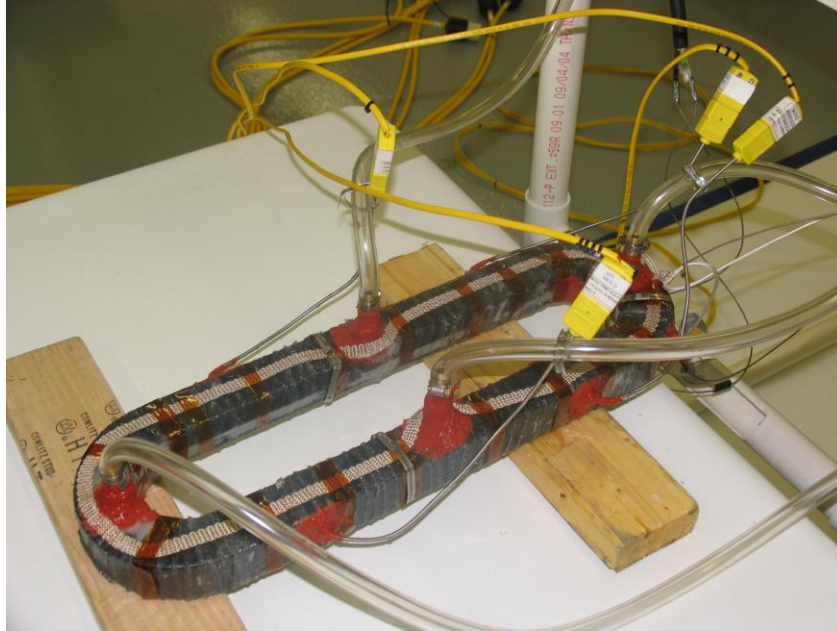


Fig. 3.1.2: Coil wound on the form. It is sealed with tapes and connected to tubes leading to vacuum pump and is ready for epoxy (CTD 403) impregnation

The conductor was then impregnated with CTD 403 Cyanate Ester (supplied by Composites Technology Development Corporation) using the vacuum pressure impregnation (VPI) technique. Curing was carried out according to the cure cycle suggested by the CTD 403 manufacturer (Composite Technology Development, Inc.). The cure cycle used was 1) Ramp temperature from 40°C to 110°C for 9 hours. The circular coil must be monitored during the cure cycle to assure leakage of epoxy does not occur and temperatures remain constant. 2) Hold at 110°C for 8 hours for post cure. 3) Ramp temperature from 110°C to 150°C for 4 hours. 4) Hold temperature of 150°C for 4 hours. 5) Ramp temperature from 150°C to 175°C for 2 hours. Once the epoxy cure temperature of 175°C was met, the temperature must remain constant for the entire cure cycle for a period of 4 hours. Following the cure cycle, turn off all heating elements and allow the circular coil to cool down naturally and the cure cycle is illustrated in Fig.3.1.3. The copper/polymer volume fraction was about 78/22 in the conductor. The final test coil after vacuum impregnation and removal of insulation tapes is shown in Fig. 3.1.4.

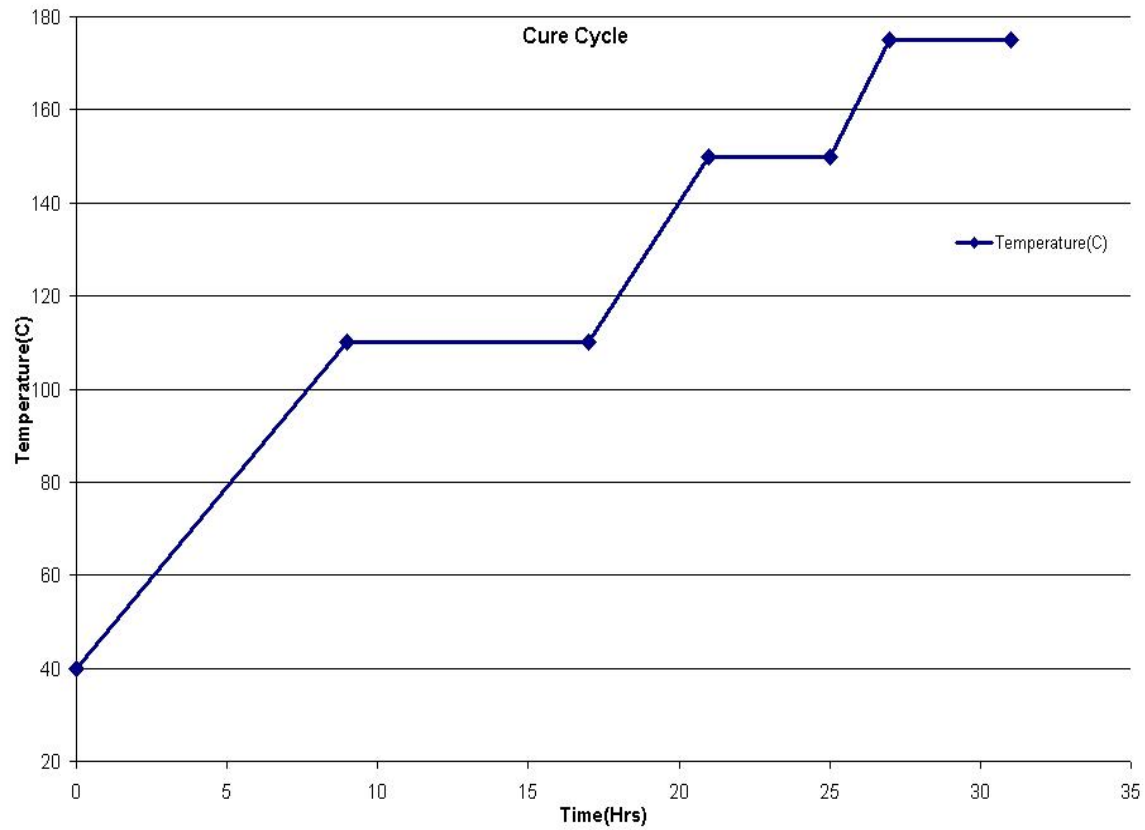


Fig. 3.1.3: Cure cycle used for the conductor as described by CTD 403 manufacturer.



Fig. 3.1.4: Test coil after vacuum impregnation

The objective of the experiments was to investigate the cooling behavior of the conductor for various flow rates when cooled from different temperatures. For this purpose six locations along the conductor length were sand cleaned using first a 200 grit sand paper and then a 400 grit sand paper to expose copper strands. Thermocouples were securely taped at these locations ensuring that the thermocouple tips were in contact with exposed copper strands. These locations were at 0.8 ft (4.5%), 4.5 ft (25%), 6.3 ft (35%), 9.9 ft (55%), 13.5 ft (75%), and 17.6 ft (95%) from inlet; as shown in Figure 3.1.5. In addition, one thermocouple was placed at the exit port on the copper tube to record the exit water temperature. The other ends of the thermocouples were connected to an eight-channel OMEGA® data logger which read the temperature versus time data and was recorded on a computer.



Fig. 3.1.5: Conductor used for Experiments with thermocouples fixed at different locations

3.2. Experimental Design:

Experimental setup for this conductor model experienced significant changes in its design. In order to heat and then cool the conductor several iterations had to be done to obtain a meaningful experimental data. The first iteration was to use the heat tape for heating. This method, although simple to use, yielded non-uniform heating. In the second iteration, a forced air convection oven was used for heating the conductor to eliminate non-uniform heating, which resulted in irregular cooling. The third iteration was the final iteration, which yielded accurate results after applying all the changes concluded from iterations one and two. The details of these iterations are described in the following sections.

3.2.1 Iteration 1 - Heat Tape Heating

In this iteration, conductor was heated using heat tape. The heat tape was wrapped carefully along the length of the conductor with its end plugged in to the DC power supply. A total of 20 feet long tape was used having the heating capacity of 560 watts. The inlet end of the embedded copper tube was connected to the tap water via a flow meter. The water from the exit end of the embedded copper was returned to the sink via flexible tubing. The temperature of each thermocouple was controlled manually by adjusting the power input to the heat tape. After heating the conductor to a desired temperature, the tap water was allowed to flow through the embedded copper tube at a given flow rate. Figure 3.2.1 below shows the recorded cooling profile of this experimental design with the conductor temperature heated to about 60°C and the water flow rate is at 0.1GPM.

The following observations can be made from the recorded data (Figure 3.2.1):

- As we can see from Figure 3.2.1, the six thermocouples mounted on the conductor did not reach the same temperature. The maximum temperature difference between different thermocouple readings was 8°C, which was a significant variation. It was difficult to manually control the temperature of individual thermocouples. This is because the thermocouples that are closer to the heat tape are heated faster than those away from it. Another reason for non-uniform heating may be attributed to the heat loss through the insulation wrapping.

Due to these difficulties, the heat tape method of heating was abandoned.

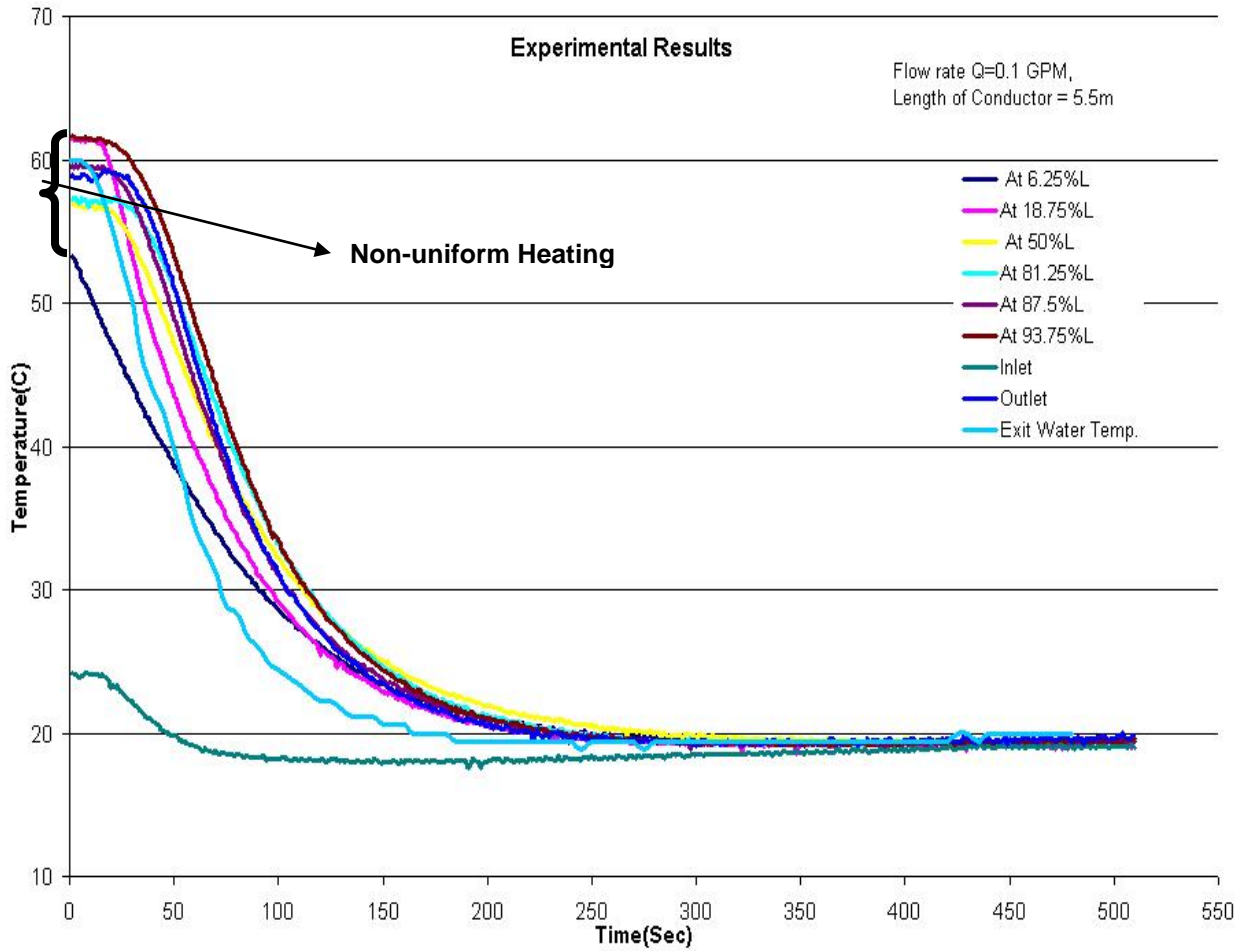


Fig. 3.2.1: Temperature Profile of Heat tape heating.

3.2.2 Iteration 2 - Forced Air Convection Heating

As the temperature control using the heat tape was difficult, forced air convection oven was used for heating the conductor. The heat tape was removed and the conductor was tightly wrapped with glass fiber insulation and placed inside the forced air convection oven. The oven has two small holes on its sides, to allow for connecting the tubing to the inlet and the outlet ports of the conductor. All the tubing outside the oven was wrapped with fiberglass insulation to minimize the heat loss from the conductor. This experimental setup is shown in Figure 3.2.2 below:

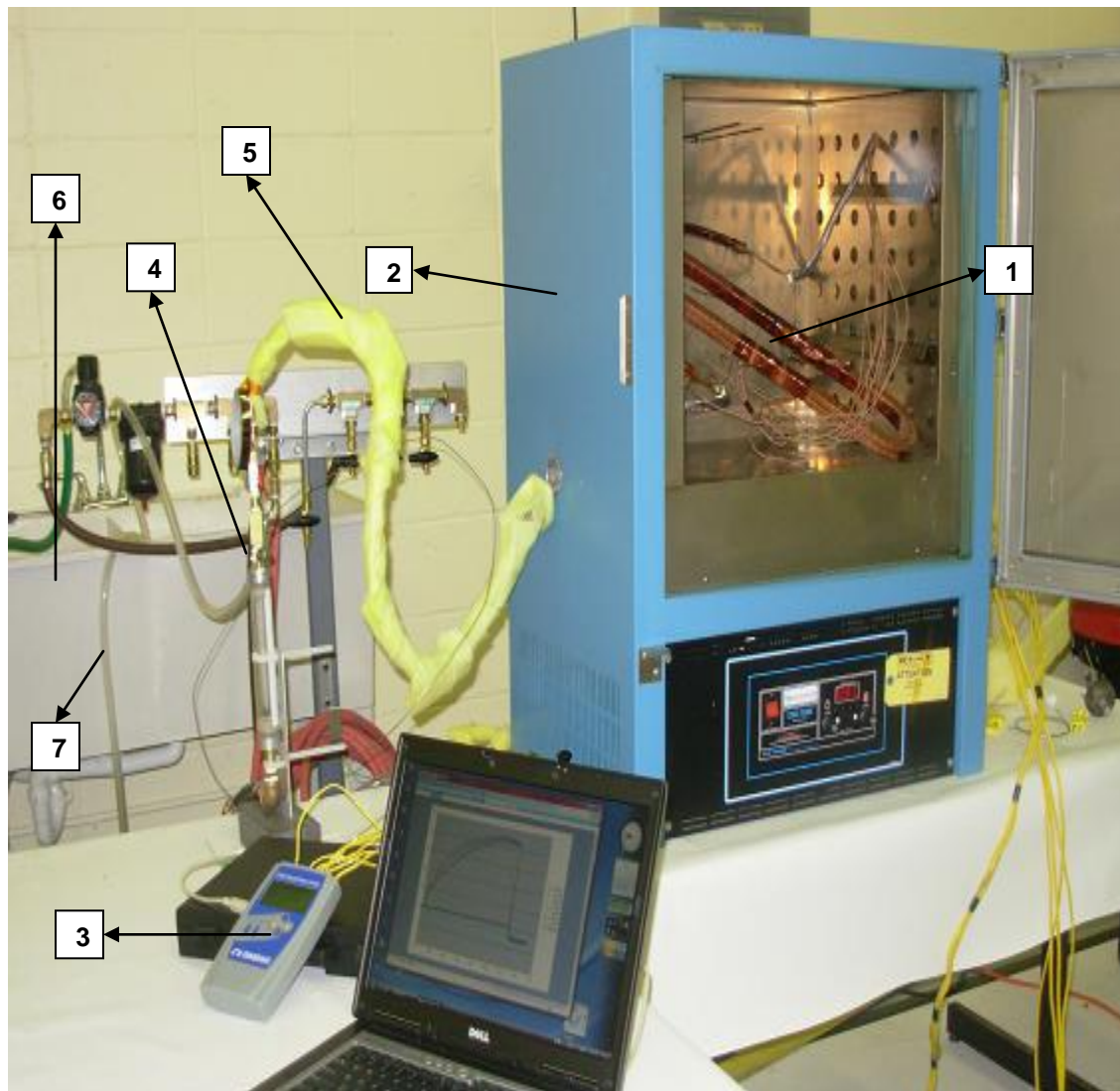


Fig. 3.2.2: Experimental setup: 1) Race track coil with thermocouples mounted; 2) Forced Air Convection Oven; 3) Data logger; 4) Flow meter to regulate the water flow; 5) Tubing with fiber glass insulation connecting the Inlet of the copper tube; 6) Water Sink, and 7) Tube allowing the water to discharge from the outlet of copper tube.

In this experiment, the temperature of the oven was set to about 63°C and oven was turned on. The temperature of the conductor was monitored during the heating process. After the temperature reached to about 62°C - 63°C, the power to the heating elements was switched off while the air circulating fan inside the oven continued to run. In about 10-15 minutes after that, the temperature of all the thermocouples converged to about 61°C. At this point water was allowed to flow at 0.1GPM to begin the cooling process. Figure 3.2.3 shows the recorded temperature-time plot for all the thermocouples.

Following observations were made from this experiment:

- While the different thermocouples took a different heating path, they all converged to one temperature. The maximum temperature difference among the thermocouples just prior to the start of cooling was less than 1°C.
- The heating and cooling curves are smoother compared to those obtained with heat tape heating (see Figure 3.2.1).

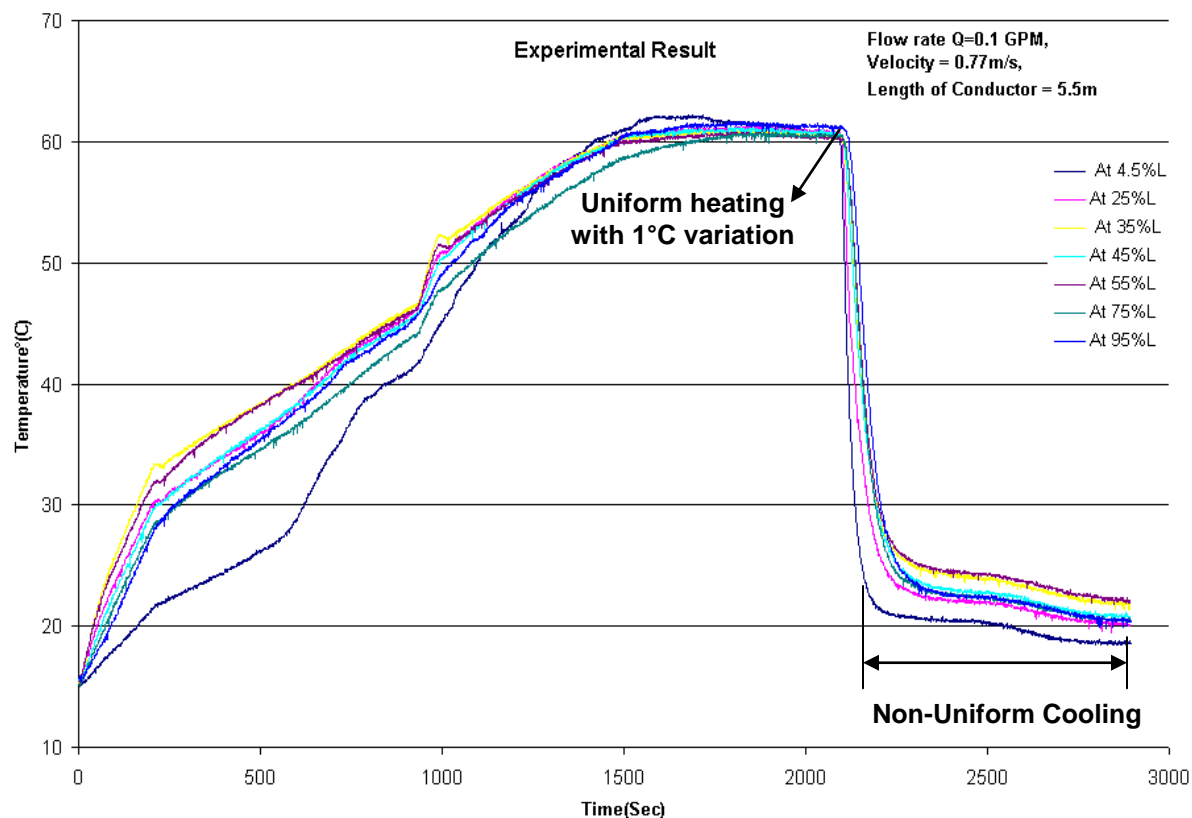


Fig. 3.2.3: Temperature profile of conductor when heated to 63°C and cooled by water flow rate of 0.1GPM using the initial experimental setup

- The only unusual observation from this experiment is that from the last leg of cooling. After the sharp drop in the conductor temperature when the cooled water is allowed to flow through the embedded copper tube, there appears to be two distinct cooling rates (Observe the “Non Uniform Cooling” in Figure 3.2.3).

The reason for this peculiar cooling behavior was suspected to be the varying inlet water temperature. In order to verify this, a thermocouple was fixed at the inlet of the copper tube (outside of the oven) to monitor the water temperature coming out of the faucet. The above experiment was repeated with the same conditions except for additional thermocouple mounted to monitor the inlet water temperature. The Figure 3.2.4 below shows the recorded data from this experiment.

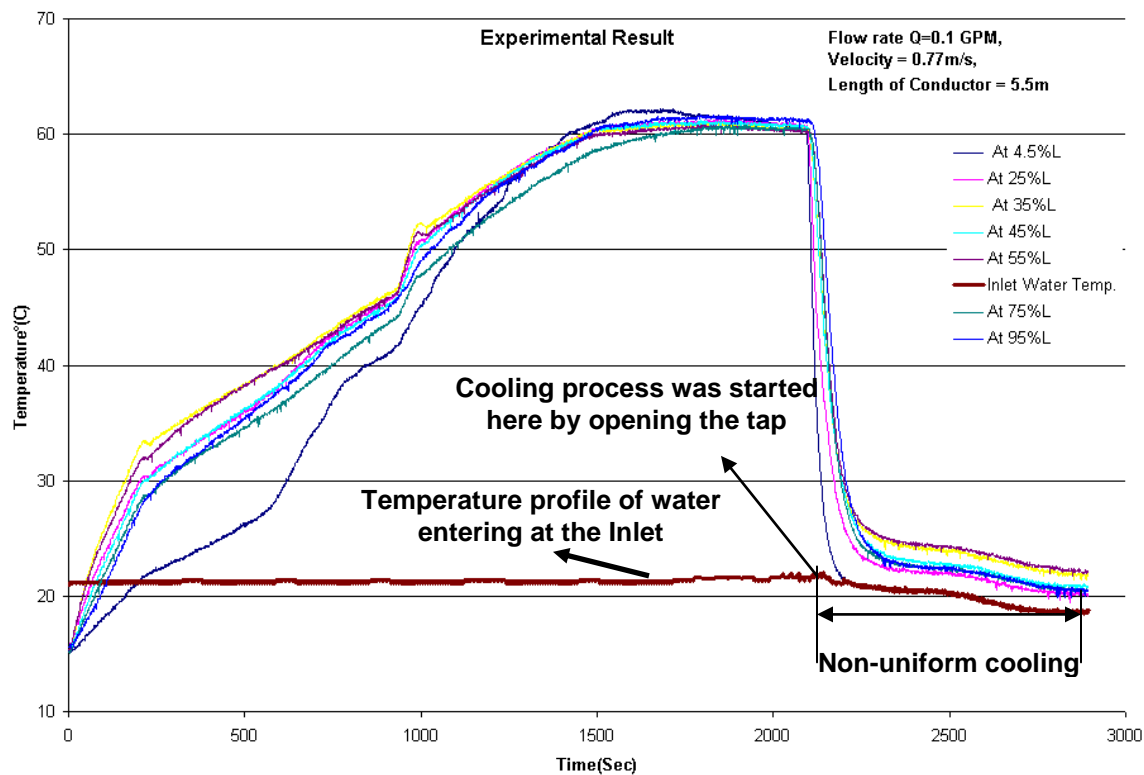


Fig. 3.2.4: Temperature profile of conductor when heated to 63°C and cooled by water flow rate of 0.1GPM using the initial experimental setup monitoring the inlet water temperature

As suspected the inlet water temperature was not constant. In fact, the last leg of cooling almost completely mirrors the temperature change in the water. Note that the tap was turned on only after the conductor reached a uniform temperature. The change in the tap water temperature can be explained as follows: These experiments were done in winter season. As the tap is turned on, the water which is already in the hoses inside the room is discharged. Since the room is heated, this water is at higher temperature than outside. As the water continues to discharge, the water sitting in the hoses outside the building reaches the tap. This water is at a lower temperature. The recorded temperature-time plot of inlet water clearly shows this behavior.

3.2.3 Iteration 3 - Final Design:

In order to correct the varying inlet water temperature, a two-way flow valve was added at the inlet between the tap and the flow meter. The purpose of the two-way valve was to let the water continue to flow at the same rate as the one used in the experiment until the water temperature stabilized before letting it in the conductor. For example, if the cooling experiment was to be run at 0.1GPM, the water was continued to be discharged back into the sink at 0.1GPM until the inlet water temperature is stabilized. Therefore, while the conductor was heating, the water was continued to be discharged back in the sink without going through the conductor. Once the conductor was heated to a given temperature, the two-way valve was adjusted to let the water go through the conductor. This process ensured that the inlet water temperature did not change while the real cooling experiment was conducted. This was the final experimental design used to perform experiments after employing all the changes from the above iterations. Experiments were conducted in which the conductor was heated to two different temperatures (60°C and 80°C) and then cooled by the room temperature water flowing through the cooling tube at five different flow rates – 0.1, 0.15, 0.2, 0.25, and 0.3 GPM.

3.3 Experimental Procedure:

The experimental procedure for conducting the cooling tests was as follows:

Warm up Procedure:

1. Turn on the data acquisition.
2. Turn on the flow and set the water at a desired flow rate. Cold tap water is allowed to flow back directly to the sink without going through the conductor using the two-way flow control valve.
3. Simultaneously, adjust the oven temperature to a couple of degrees higher than the desired value. Set the data acquisition system to record the temperature and start heating the conductor.
4. Once the oven temperature has reached to the set value, turn off the oven heater while leaving the fan on. Monitor the temperature from all the thermocouples, and when all the thermocouples converged to a single temperature ($\pm 1^{\circ}\text{C}$), turn the fan off and adjust the two-way valve to direct the water into the cooling tube at the already set flow rate. Monitor the system for any leaks, air bubbles, and temperature reading of the thermocouples.

In all the experiments, temperature was recorded at 1-second time intervals for all the eight thermocouples during the heating and cooling of the conductor. A typical result obtained for a flow rate of 0.15 GPM and the conductor temperature heated to 63°C is shown in Figure 3.3.1 and the remaining results were shown in the Appendix A.

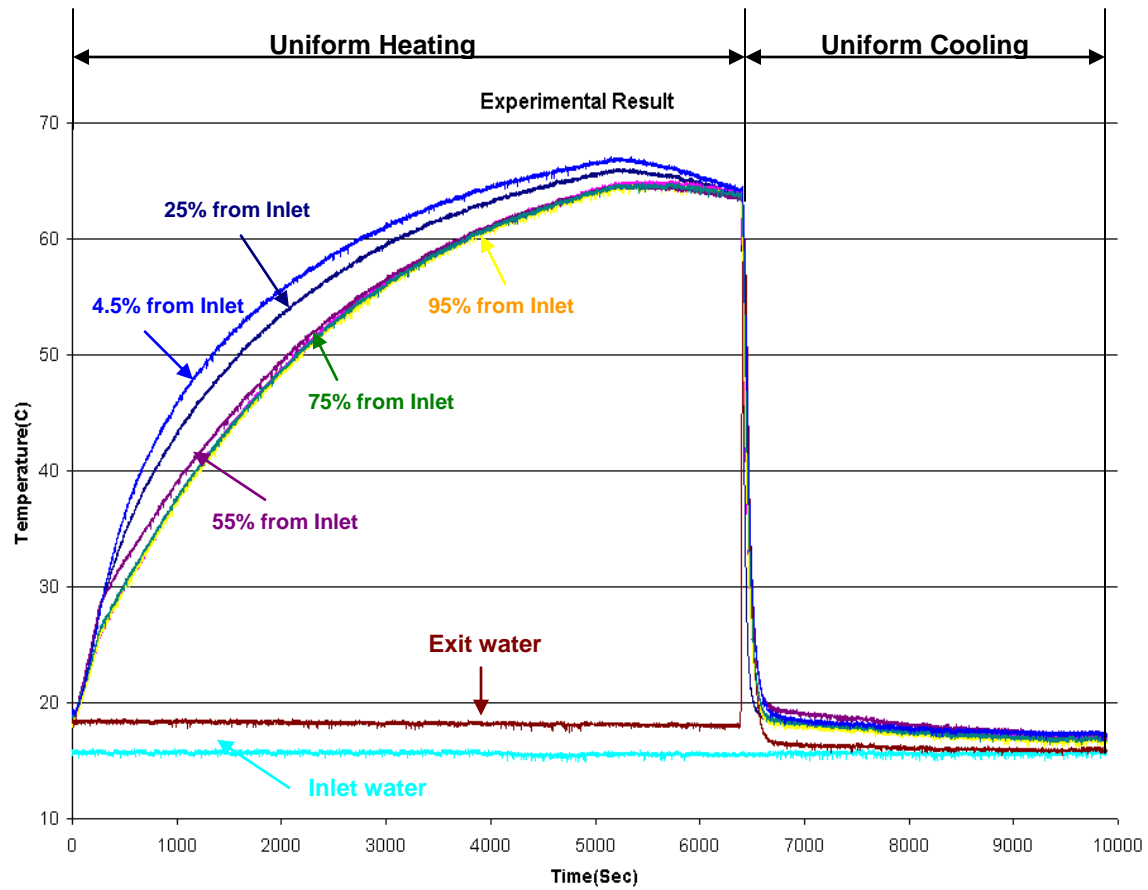


Fig. 3.3.1: A typical result obtained when conductor was heated to 63°C and cooled by flow rate of 0.15 GPM with the Final Experimental design.

4. Numerical Simulation:

Heat Transfer analysis of the conductor (18ft) was numerically simulated in Matlab© software using the Lumped transient method. The objectives of the study were to predict the cooling behavior for long conductors, compare the predictions with the experimental results obtained from 18-ft long conductor and then apply the model to predict the cooling behavior of the full length (120ft) QPS conductor.

4.1. Elemental Approach / Lumped Transient Model:

In this elemental approach, the 0.45 in x 0.45 in square conductor shown in Fig.2.1.1 was modeled as a circular conductor such that its cross-sectional area is same as that of the square conductor as shown in Figure 4.1.1. The copper tube in the middle was modeled as a 3/16" diameter hole.

The composite and water are divided into equal number of elements of uniform length along the length of the conductor as shown in Fig. 4.1.2. Each water element undergoes heat transfer with each of the composite element as it moves in the tube from inlet to outlet. It was assumed that the water elements stop for a very small time (called time step) for the heat transfer with the composite element as it moves towards the outlet. The duration of the time step is related to the water flow velocity. The conductive heat transfer between a water element and all composite elements happens sequentially and continuously until the water element exits the tube.

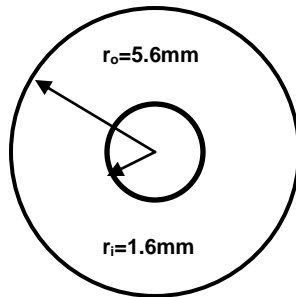


Figure 4.1.1: Square conductor modeled as a circular conductor.

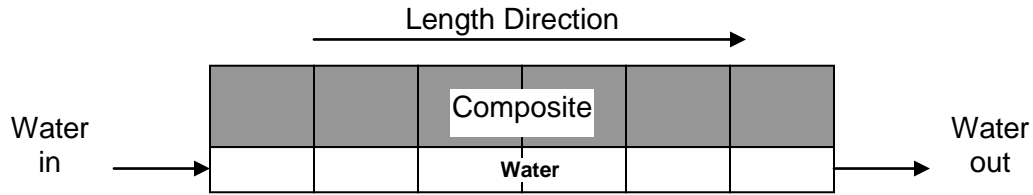


Fig. 4.1.2: Elemental approach

When the first water element, which is initially at temperature T_{iW} , enters the tube and interacts with the first composite element, which is initially at temperature T_{iC} , for the duration of the time step, heat is removed from the composite element and added to the water element. The same water element, which is now at a higher temperature than T_{iW} , interacts with the next composite element. Simultaneously, fresh water elements at temperatures T_{iW} continue to enter the tube and interact with composite elements, and the process continues until conductor is cooled to a desired temperature.

We first assume that there is no temperature gradient in the radial direction in the composite, i.e. at every instant during each time step; the temperature is same throughout the entire composite element. We also assume that there is no heat transfer between the neighboring composite or water elements. Adiabatic boundary conditions were also assumed, i.e. there is no heat exchange across the outside surfaces of the composite. The temperature of the elements of the composite conductor at the end of each time step is calculated using the Lumped Transient method [15] as described below.

Heat transfer is driven by a temperature difference between an object and its surroundings. Heat transfer is dependent upon both the internal resistance (L/kA) and surface resistance ($1/hA$). There is a class of problems for which the convective resistance at the surface boundary is large compared to the internal resistance due to conduction. For solids of large thermal conductivity with surface areas that are large in proportion to their volume, the internal resistance can be assumed to be negligible in comparison with the convective resistance at the surface. The process in which internal resistance is ignored being negligible in comparison with its surface resistance is called the Newtonian Heating or cooling process. In this process the temperature throughout the solid is considered to be uniform at a given time. Such an

analysis is also called Lumped Heat Capacity Analysis because the whole solid, whose energy at any time is a function of its temperature and total heat capacity is considered as one lump. The QPS conductor was modeled using the same lumped transient approach in which each composite element is considered as one lump. The internal resistance of each composite element is considered to be negligible. The temperature of a body using Lumped Transient method is derived below:

Consider a solid of area A (m^2) whose initial temperature is T_{ic} throughout and which is suddenly placed in a new environment at a constant temperature T_{iw} .

The lumped heat capacity of the solid is ρcV , where ρ (kg/m^3) is density of solid;

C_{p_c} ($\text{J}/\text{kg}\cdot\text{K}$) is the specific heat of the solid and V (m^3) is the volume of solid. The convective heat transfer coefficient between the solid and the surroundings is h ($\text{W}/\text{m}^2\cdot\text{K}$). At any instant of time, t , the convective heat loss from the body is equal to the decrease in internal energy of the solid.

Thus,
$$Q = -hA(T - T_{iw}) = \rho cV \frac{dT}{dt} \quad (1)$$

Rewriting eq. (1),
$$\frac{dT}{T - T_{iw}} = \frac{-hA}{\rho cV} dt \quad (2)$$

Integrating eq. (2), we get
$$\ln(T - T_{iw}) = \frac{-hA}{\rho cV} t + C_1 \quad (3)$$

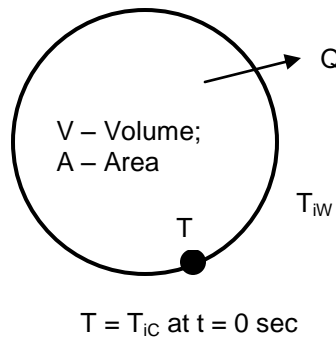


Figure 4.1.3: Lumped Heat Capacity System

The constant of integration, C_1 can be found by applying the initial condition, $T = T_{iC}$ at $t = 0$ sec which gives $C_1 = \ln(T_{iC} - T_{iW})$. Substituting the value of C_1 in eq. (1), we get

$$\ln \frac{(T - T_{iW})}{(T_{iC} - T_{iW})} = \frac{-hA}{\rho c V} * t \quad (4)$$

$$\frac{(T - T_{iW})}{(T_{iC} - T_{iW})} = \exp \left[- \left(\frac{hA}{\rho c V} \right) * t \right] \quad (5)$$

The parameter $\left(\frac{hA}{\rho c V} \right) * t$ can be rewritten as follows:

$$\left(\frac{hA}{\rho c V} \right) * t = \left(\frac{A}{V} \right) \left(\frac{h}{\rho c} \right) \left(\frac{kL_c}{kL_c} \right) * t = \left(\frac{hL_c}{k} \right) \left(\frac{kt}{\rho c L_c^2} \right) = \left(\frac{hL_c}{k} \right) \left(\frac{\alpha t}{L_c^2} \right) = Bi.Fo$$

Where $\left(\frac{hL_c}{k} \right) = Bi$, is the Biot number.

Biot number is the ratio of internal resistance to convective resistance. Biot number is a non-dimensional parameter. L_c is the characteristic length and is equal to the ratio of the volume of the body to its surface area involved in the heat transfer. While modeling the QPS conductor L_c is taken as

$$L_c = \frac{Volume}{Surface.area} = \frac{\pi * (r_o^2 - r_i^2) * height}{\pi * r_o * height} = \frac{(r_o^2 - r_i^2)}{r_o} \quad (6)$$

$\alpha = \left(\frac{k}{\rho c} \right)$, is the thermal diffusivity; $\left(\frac{\alpha t}{L_c^2} \right) = Fo$, is the Fourier number.

$$\therefore \frac{(T - T_{iW})}{(T_{iC} - T_{iW})} = \exp[-Bi * Fo] \quad (7)$$

The above equation gives the temperature distribution as a function of time for a solid initially at a temperature, T_{iC} , which is placed in a convective environment at a temperature of T_{iW} . The final temperature of the water element T_f , after reacting with the composite element was calculated using the law of conservation of energy as follows:

$$-m_c * C_{p_c} * (T_{iC} - T_f) = m_w * C_{p_w} * (T_{iW} - T_f) \quad (8)$$

where T_f is the final temperature of water; m_c and m_w are the masses of composite and water elements, respectively and Cp_c , and Cp_w are the heat capacities of composite and water elements, respectively.

To understand how this works for modeling in the QPS conductor, consider the inlet end of the tube. When one water element enters the tube say at $T_{iw}=20^\circ\text{C}$ (68°F), change in temperature of water element was calculated by conservation of heat for each time step, i.e. the heat lost by the composite element is same as the heat gained by the water element (Fig. 4.1.4). This is the initial temperature of water element in contact with 2nd composite element at next time step. Another water element at 20°C (68°F) enters the tube at the same instant and the 1st composite element is at the lower temperature than the initial. This happens across the tube length for a given length of time.

T_{ic} is the initial temperature of composite (60°C or 140°F at time = 0)

T_{iw} is the initial temperature of water (20°C or 68°F at time = 0)

From the equation (7), the final temperature T of the composite will be calculated.

This water element with the increased temperature moves to the next position and interacts with the 'already' cooled composite element based on the same assumptions.

This process continues as fresh water elements at a prescribed temperature and velocity continue to enter from the inlet and interact with previously cooled composite elements. The algorithm for the lumped transient approach was developed in MATLAB-7©.

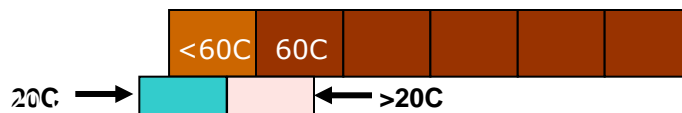


Fig. 4.1.4: Movement of elements

The omission of the radial temperature gradient in the composite element implies that the resistance to conduction inside the composite element is much smaller than the resistance to convection outside. Thus a convection problem is transformed into a conduction problem using the lumped method. The model thus becomes a conduction model and the temperatures predicted by this model should give an envelope beyond which cooling is not possible. Table 4.1 below gives some of the constant values used in the lumped transient model algorithm. The physics of the model discussed till here was developed by Shankar [17] and the following sections describe the further changes added to the model.

Radius of the copper tube r_i	$1.6 * 10^{-3} m$
Radius of the composite r_o	$5.6 * 10^{-3} m$
Cross sectional area A	$\pi * r_i^2 = 0.0082 * 10^{-3} m^2$
Conductivity of the composite k_c	9.9 W/m-K
Characteristic length $L_c \left(\frac{Volume}{Surface.area} \right)$	$\frac{\pi * (r_o^2 - r_i^2) * height}{\pi * 2 * r_o * height} = \frac{r_o^2 - r_i^2}{2 * r_o}$ $= \frac{0.0056433^2 - 0.001619^2}{0.003239} = 0.00902m$

Table 4.1: Values used in the Lumped Transient Model algorithm.

4.2. Biot number calculation:

The Biot number is defined as the ratio of thermal internal resistance and surface film resistance. The omission of the thermal gradient in composite elements implies that the surface film resistance (h) is much larger than internal thermal resistance (k/L_c).

$$Bi = \left(\frac{hL_c}{k} \right) \quad (9)$$

The convective heat transfer coefficient (h) value is obtained from the Nusselt number using the Gnielinski correlation [18, 19].

$$Nu = \frac{(f/8) * (Re - 1000) * Pr}{1 + (12.7 * \sqrt{(f/8)} * (Pr^{(2/3)} - 1))} = \frac{hD}{k_w} \quad (10)$$

where Re – Reynolds number; Pr - Prandtl number; k_w - Thermal conductivity of water; D – Diameter of the copper tube = $2 * r_i$, and f is called the Darcy friction factor defined by Petukhov formula [20] as follows:

$$f = \frac{1}{[0.790 * \ln(Re) - 1.64]} \quad (11)$$

The Gnielinski equation applies for ranges of Prandtl number between 0.5 and 10^6 ($Pr \neq 1$) and Reynolds number range of 3,000 – $5 * 10^6$. For all the data used in this research the Reynolds number ranged from 3,474 to 11,878 and Prandtl number used were 4.79 and 4.15 at water temperature of 60°C and 80°C, respectively. The calculations for these numbers are given in the Appendix C. The Biot numbers calculated for the flow conditions used in this research range from 8-11, which obviously were too large to justify the basic assumption (i.e. no thermal gradient in the composite elements) of the lumped analysis. However, if the cooling predictions are still made (using the calculated Biot Number = 10.75) for an 18-ft long conductor, the results shown in Figure 4.2.1 are obtained.

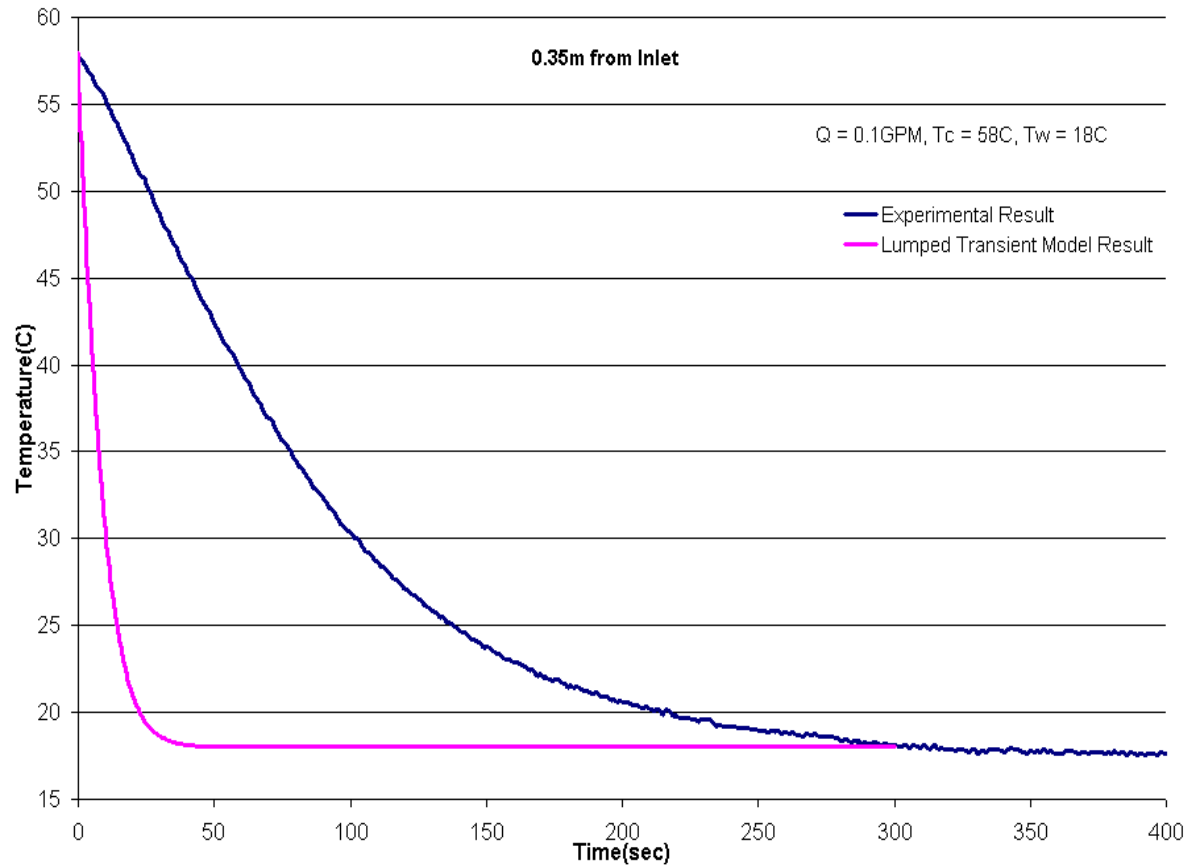


Fig 4.2.1: A typical comparison between the Experimental and Lumped transient model result.

As expected, the predicted curve produces a much rapid cooling than that observed experimentally. While the use of the lumped analysis for Biot number larger than 1 is not justified, Figure 4.3.1 does indicate that the thermal gradient in copper composite elements must be accounted for. One possible approach could be to modify the surface film resistance by introducing a radial heat resistance term.

4.3. Introduction of Heat resistance parameter:

The large Biot numbers are the result of omission of modeling of the thermal gradient in the composite elements. One of the ways the effect of the thermal gradient can be incorporated is by introducing an additional radial heat resistance term to the film resistance:

$$\frac{1}{h_e} = \frac{1}{h} + \frac{L^*}{k_c} \quad (12)$$

In the calculation of Biot number, the heat transfer coefficient h for the surface is replaced by the overall heat transfer coefficient h_e , which includes an internal resistance term L^*/k_c . In effect L^* can be considered as the distance to the centroid of the heat distribution from the cooling surface. The radial heat resistance parameter L^* was determined by curve-fitting the experimental data on cooling of the 18-ft long conductor. The L^* value of 0.009m provided the best curve fit with the experimental data. The effective convective heat transfer coefficient obtained is then used for calculating the new Biot number as:

$$Bi = \left(\frac{h_e L_c}{k} \right) \quad (13)$$

The Biot numbers calculated using the above equation ranged from 0.71 to 0.83.

5. Results and Discussion:

The results of the Lumped transient model numerically simulated in MATLAB© were compared with the experimental results. These results are presented in detail in this section. The value of the heat resistance length parameter L^* was calculated empirically by best fitting an arbitrarily selected experimental cooling data curve. This data curve was for cooling from 60°C at water flow rate of 0.2 GPM and at a location on conductor at 9.9-ft from its inlet. The L^* value obtained from this curve was 0.009 m. Then the same L^* was used to predict the cooling curves for all other combinations of flow rate, maximum temperature, and thermocouple locations along the conductor length.

5.1. Comparison between Experimental and Lumped Transient Model Results:

The cooling curves were recorded at six different locations along the conductor length for different combinations with two values of maximum temperatures (63°C and 84°C) and five different flow rates (0.1, 0.15, 0.2, 0.25, and 0.3 GPM). The algorithm for predicting the cooling curves using the Elemental approach/Lumped Transient method described in section 3 is defined in the Appendix B. The numerical computation for each case was carried out by dividing the 18-ft long conductor into 1000 equal segments. Using larger than 1000 segments did not change the results significantly. The difference between the results obtained with 10,000 and 1000 segments was less than 1%. The difference between the results obtained for 1000 segments and less than it (900, 800, and 500) was significant with a difference varying from 5% to 10%. Starting with the initial temperature of the entire conductor (60°C or 80°C), the MATLAB© code was run until the entire conductor cooled down to the within 1°C of the inlet water temperature. The thermal properties of Cu/Cyanate Ester composite conductor were determined experimentally at the High Temperature Materials Testing Laboratory (HTML) of Oak Ridge National Laboratory [21].

The comparison of the experimentally recorded and predicted cooling curves was done for five different flow rates (ranging from 0.1 to 0.3 GPM), two different initial temperatures of the conductor (60°C and

80°C), and at four different locations along the conductor lengths. In addition, the experimentally measured and predicted exit water temperatures versus time curves were also compared. Thus, a total of 48 predicted curves were compared with experimentally recorded data. In all cases, one value of the radial heat resistance parameter, L^* (= 9 mm) was used. Figures 5.1- 5.12 show representative results from these comparisons.

Table 5.1 - Properties used in the model

Property	Composite Conductor	Water
Density (Kg/m^3)	7400	1000
Thermal Conductivity, (W/(m.k))	9.9*	0.625
Specific Heat (J/(Kg.K))	404	4200
Prandtl Number at 60°C	-	4.793
Prandtl Number at 80°C	-	4.15
Kinematic Viscosity of Water (60°) (m^2/s)	-	$7.138(10^{-7})$
Kinematic Viscosity of Water (80°) (m^2/s)	-	$6.264(10^{-7})$

*In the radial direction, i.e. in the direction perpendicular to the water flow direction.

Conductor Length = 5.5 m, Water Flow Rate = 0.1 GPM
 Conductor Initial Temperature = 62°C, Water Inlet Temperature = 18°C

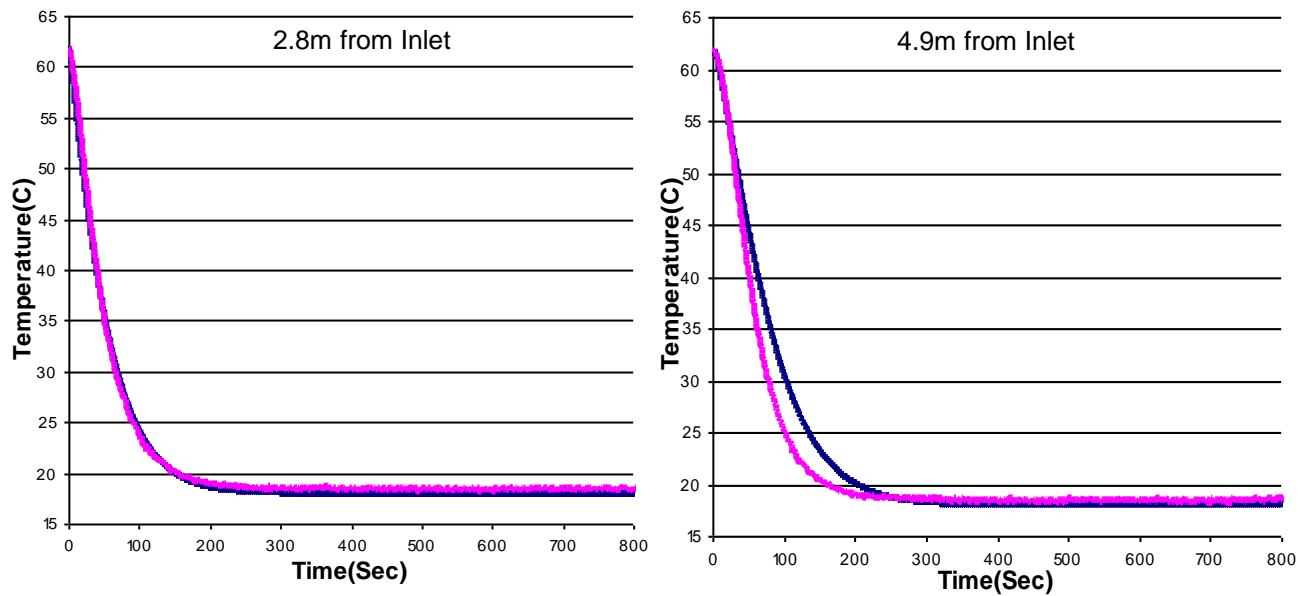
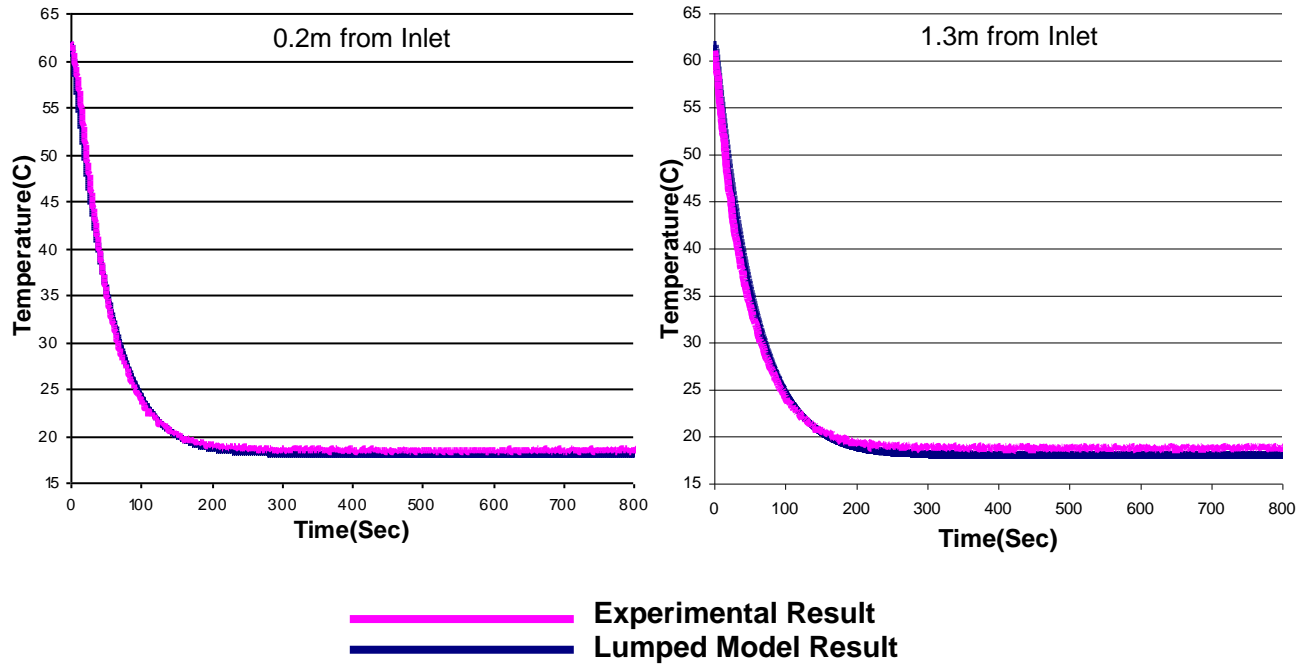


Figure 5.1: Comparisons between experimental and predicted cooling curves for 5.5 m long conductor cooled by 18°C water flowing through the cooling tube at a rate of 0.1 GPM. In all predictions, the radial heat resistance parameter (L^*) was chosen to be equal to 9 mm.

**Conductor Length = 5.5 m, Water Flow Rate = 0.15 GPM
Conductor Initial Temperature = 61.4°C, Water Inlet Temperature = 19°C**

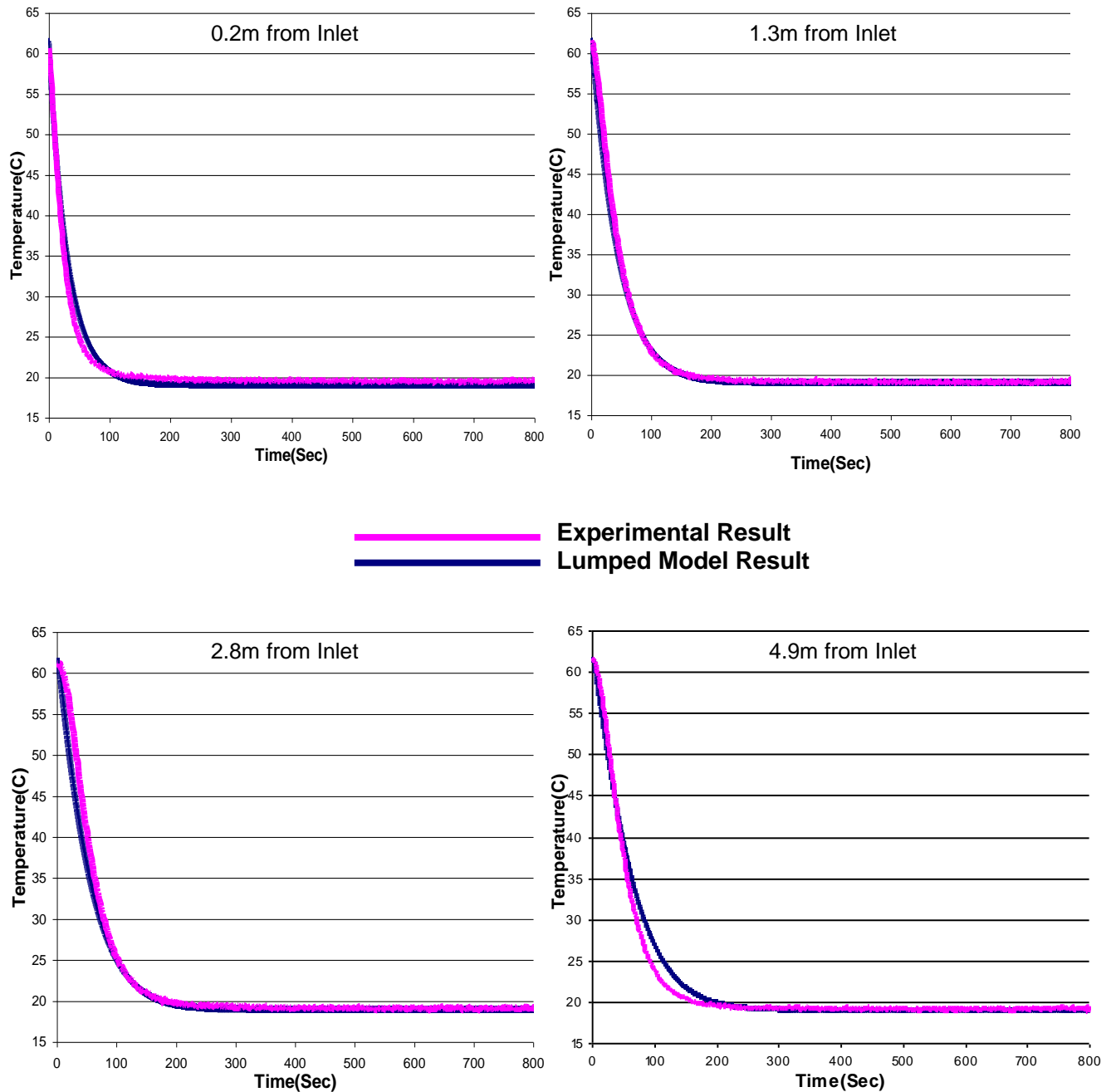


Figure 5.2: Comparisons between experimental and predicted cooling curves for 5.5 m long conductor cooled by 19°C water flowing through the cooling tube at a rate of 0.15 GPM. In all predictions, the radial heat resistance parameter (L^*) was chosen to be equal to 9 mm.

Conductor Length = 5.5 m, Water Flow Rate = 0.2 GPM
Conductor Initial Temperature = 62.37°C, Water Inlet Temperature = 18.36°C

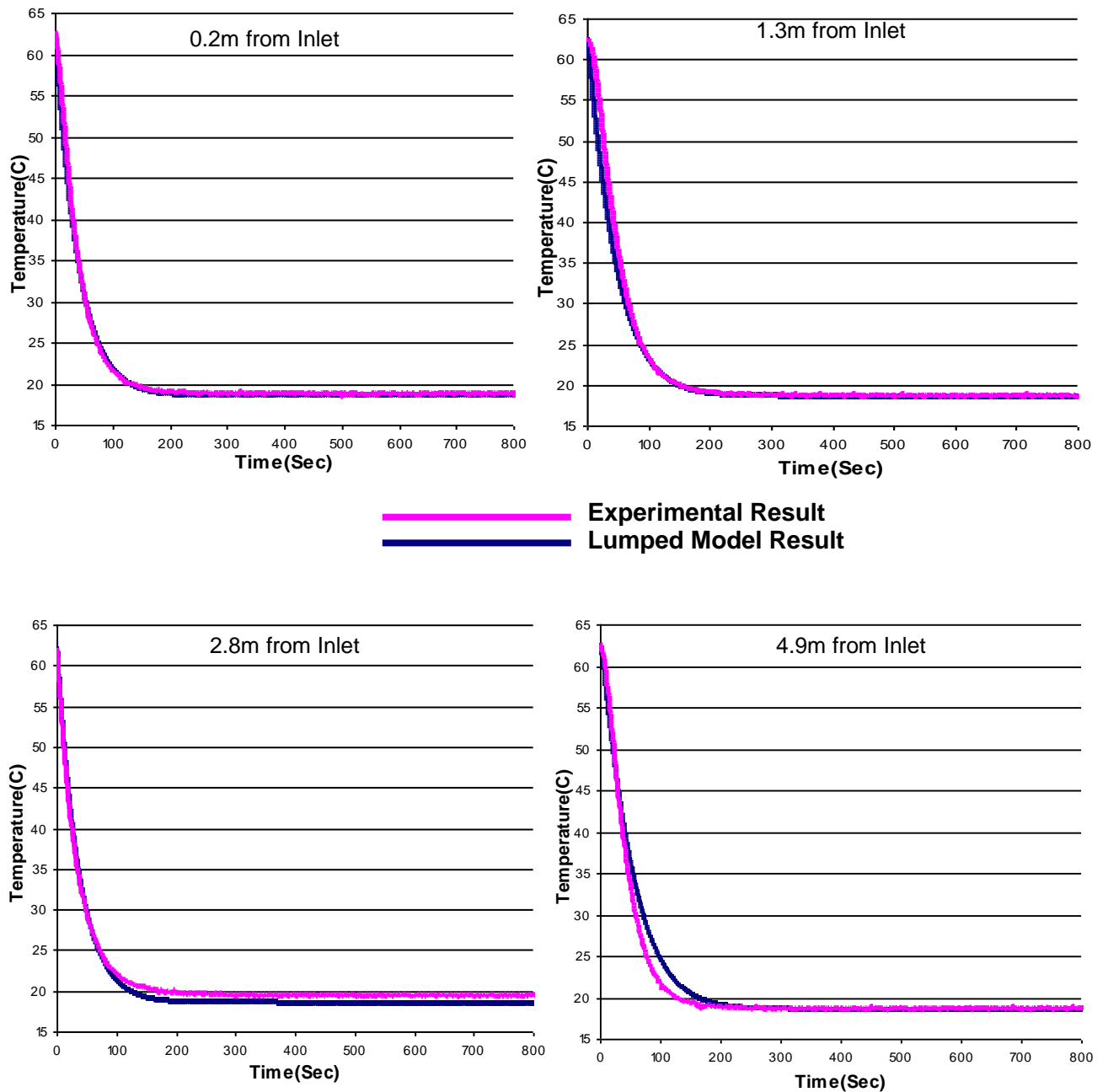


Figure 5.3: Comparisons between experimental and predicted cooling curves for 5.5 m long conductor cooled by 18.6°C water flowing through the cooling tube at a rate of 0.2 GPM. In all predictions, the radial heat resistance parameter (L^*) was chosen to be equal to 9 mm.

**Conductor Length = 5.5 m, Water Flow Rate = 0.25 GPM
Conductor Initial Temperature = 62.76°C, Water Inlet Temperature = 18.8°C**

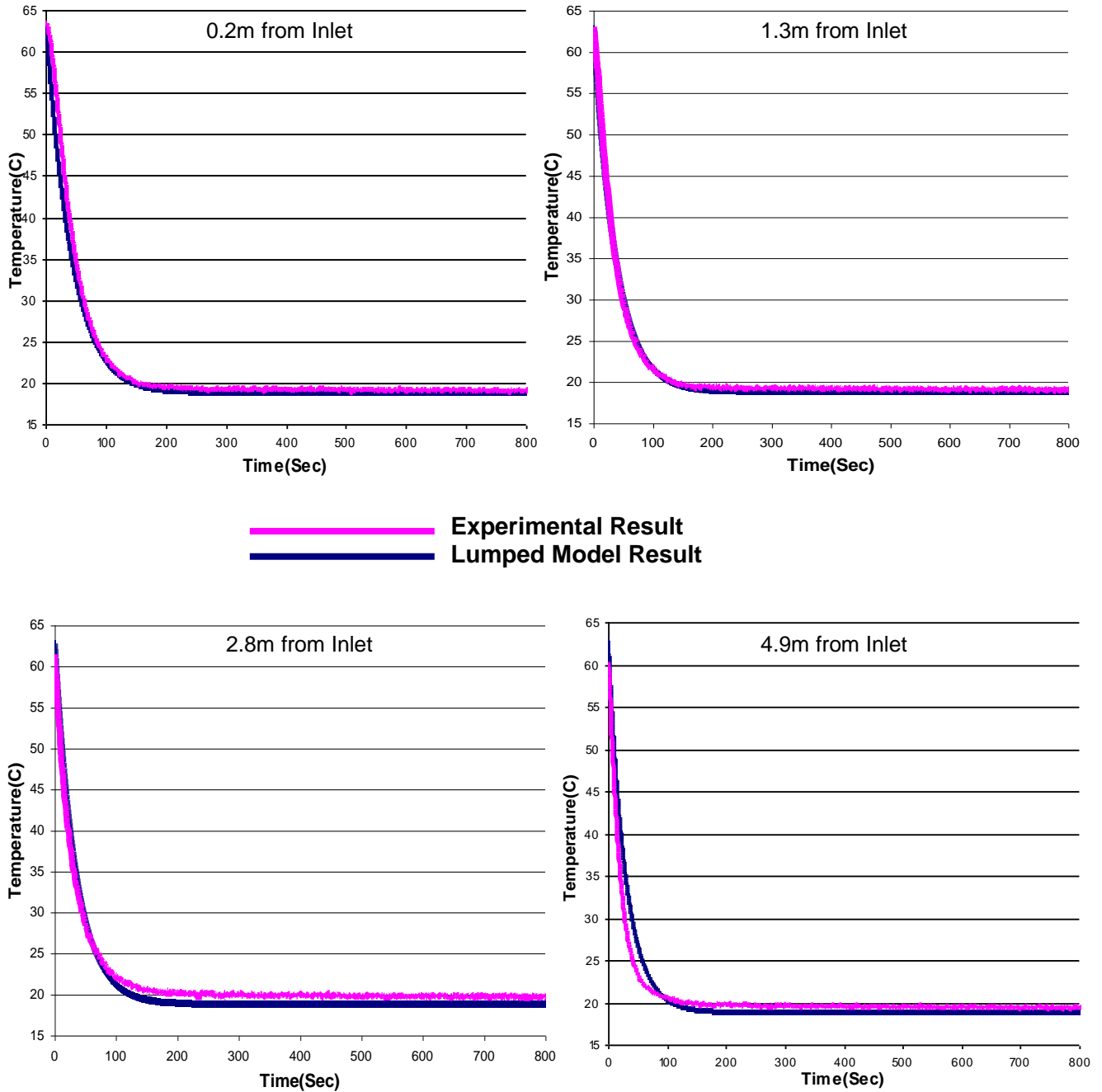


Figure 5.4: Comparisons between experimental and predicted cooling curves for 5.5 m long conductor cooled by 18.8°C water flowing through the cooling tube at a rate of 0.25 GPM. In all predictions, the radial heat resistance parameter (L^*) was chosen to be equal to 9 mm.

**Conductor Length = 5.5 m, Water Flow Rate = 0.3 GPM
Conductor Initial Temperature = 61.2°C, Water Inlet Temperature = 14°C**

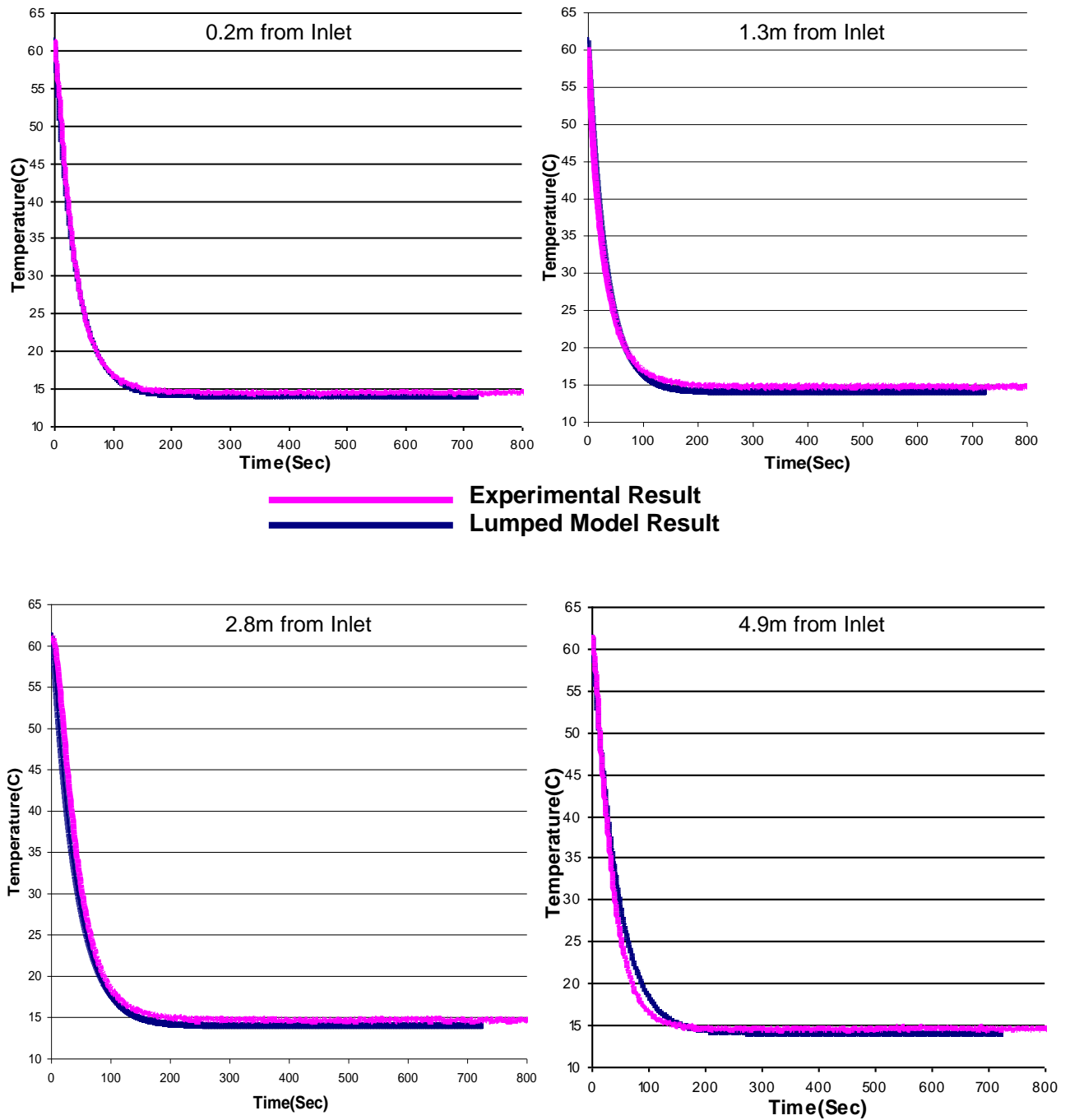


Figure 5.5: Comparisons between experimental and predicted cooling curves for 5.5 m long conductor cooled by 14°C water flowing through the cooling tube at a rate of 0.3 GPM. In all predictions, the radial heat resistance parameter (L^*) was chosen to be equal to 9 mm.

**Conductor Length = 5.5 m, Water Flow Rate = 0.1 GPM
Conductor Initial Temperature = 81.5°C, Water Inlet Temperature = 17.7°C**

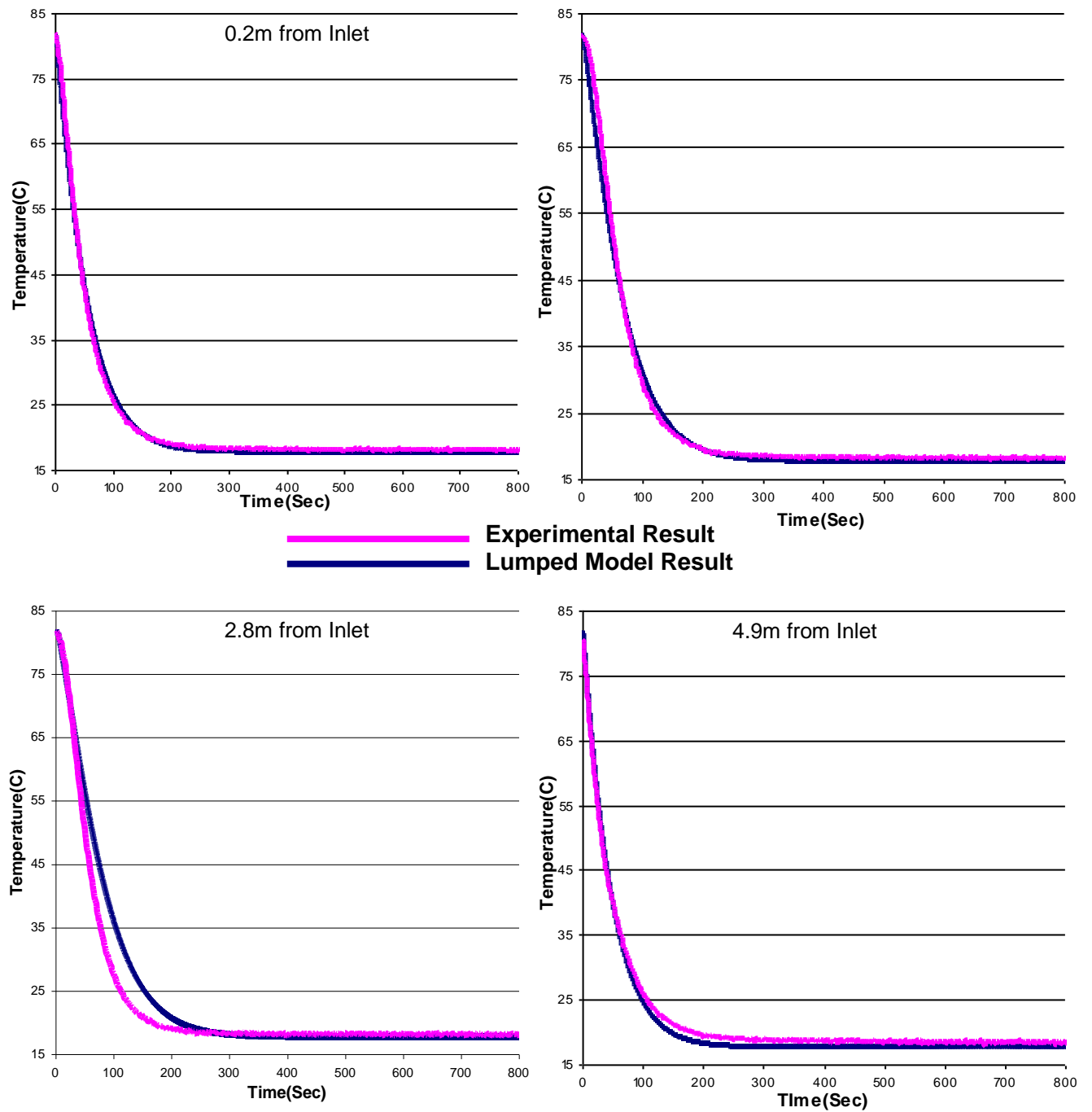


Figure 5.6: Comparisons between experimental and predicted cooling curves for 5.5 m long conductor cooled by 17.7°C water flowing through the cooling tube at a rate of 0.1 GPM. In all predictions, the radial heat resistance parameter (L^*) was chosen to be equal to 9 mm.

Conductor Length = 5.5 m, Water Flow Rate = 0.15 GPM
 Conductor Initial Temperature = 80.2°C, Water Inlet Temperature = 17°C

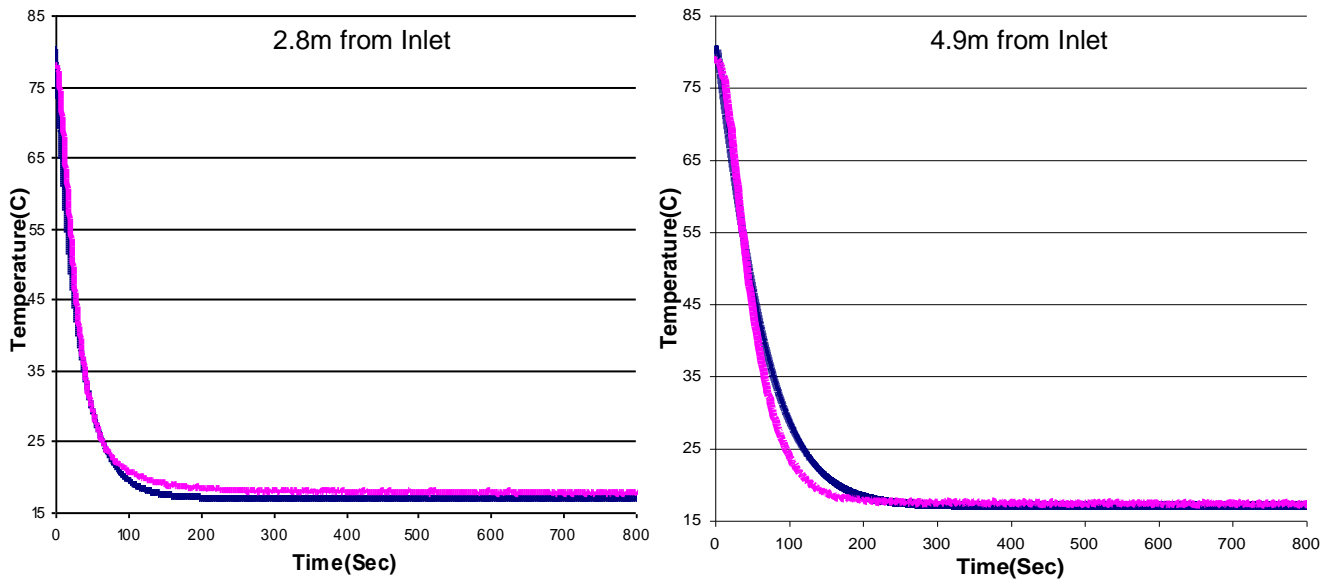
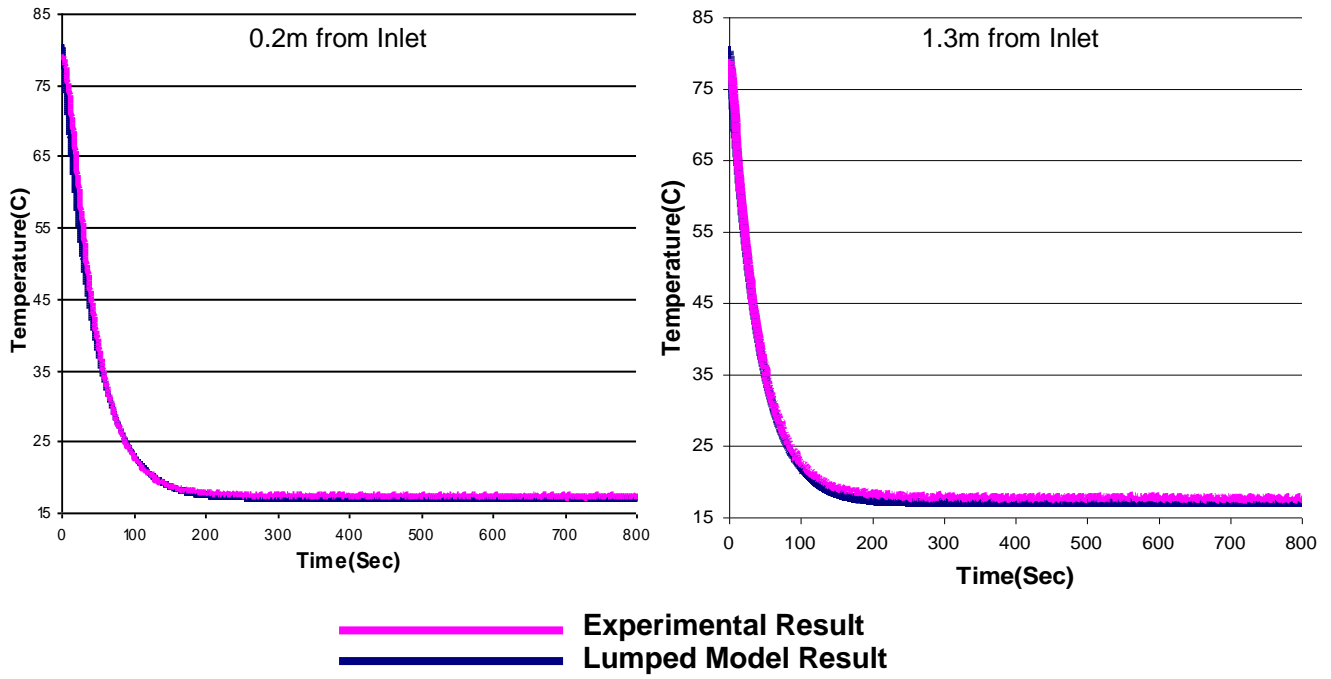


Figure 5.7: Comparisons between experimental and predicted cooling curves for 5.5 m long conductor cooled by 17°C water flowing through the cooling tube at a rate of 0.15 GPM. In all predictions, the radial heat resistance parameter (L^*) was chosen to be equal to 9 mm.

**Conductor Length = 5.5 m, Water Flow Rate = 0.2 GPM
Conductor Initial Temperature = 80.51°C, Water Inlet Temperature = 16°C**

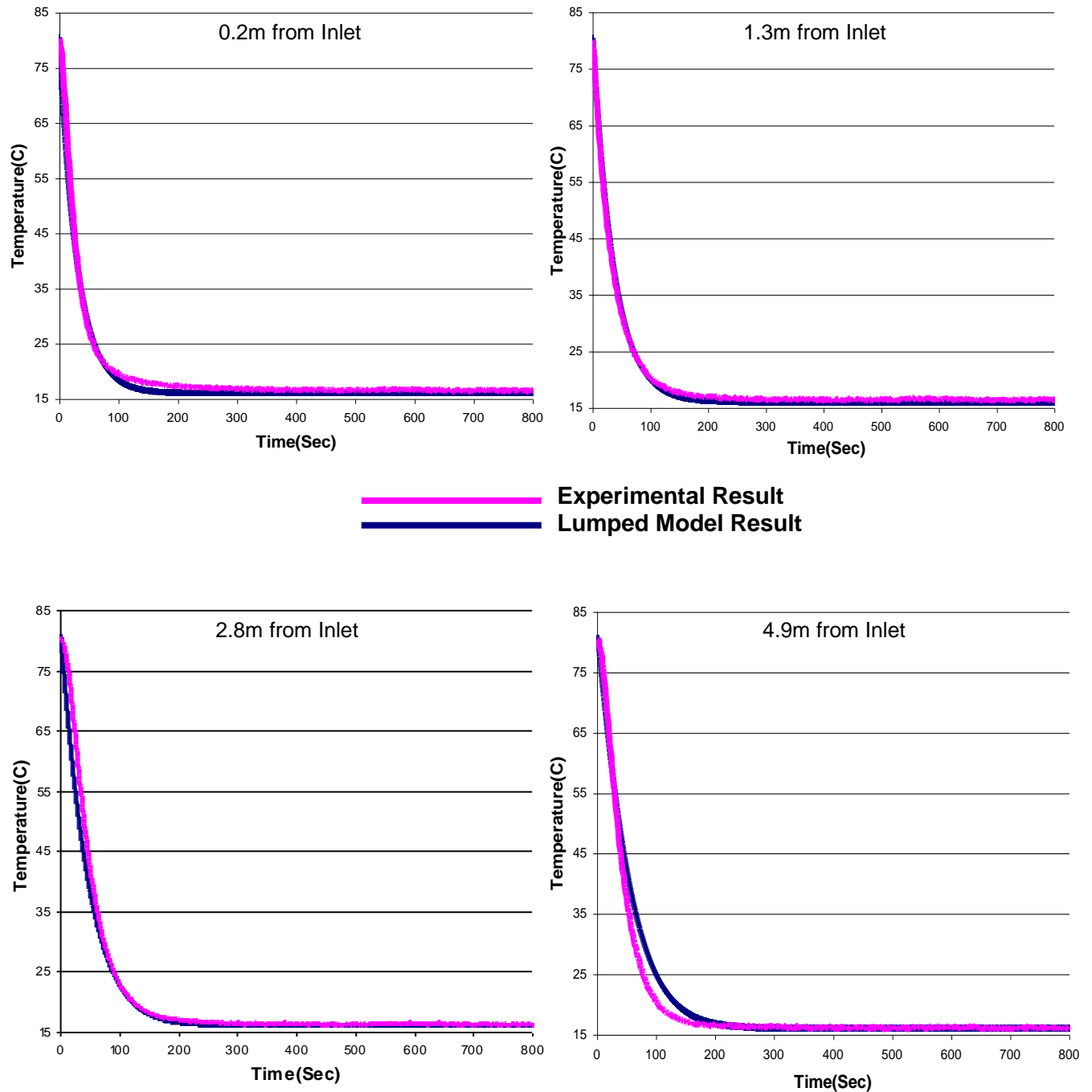


Figure 5.8: Comparisons between experimental and predicted cooling curves for 5.5 m long conductor cooled by 16°C water flowing through the cooling tube at a rate of 0.2 GPM. In all predictions, the radial heat resistance parameter (L^*) was chosen to be equal to 9 mm.

Conductor Length = 5.5 m, Water Flow Rate = 0.25 GPM
Conductor Initial Temperature = 81.042°C, Water Inlet Temperature = 15.4°C

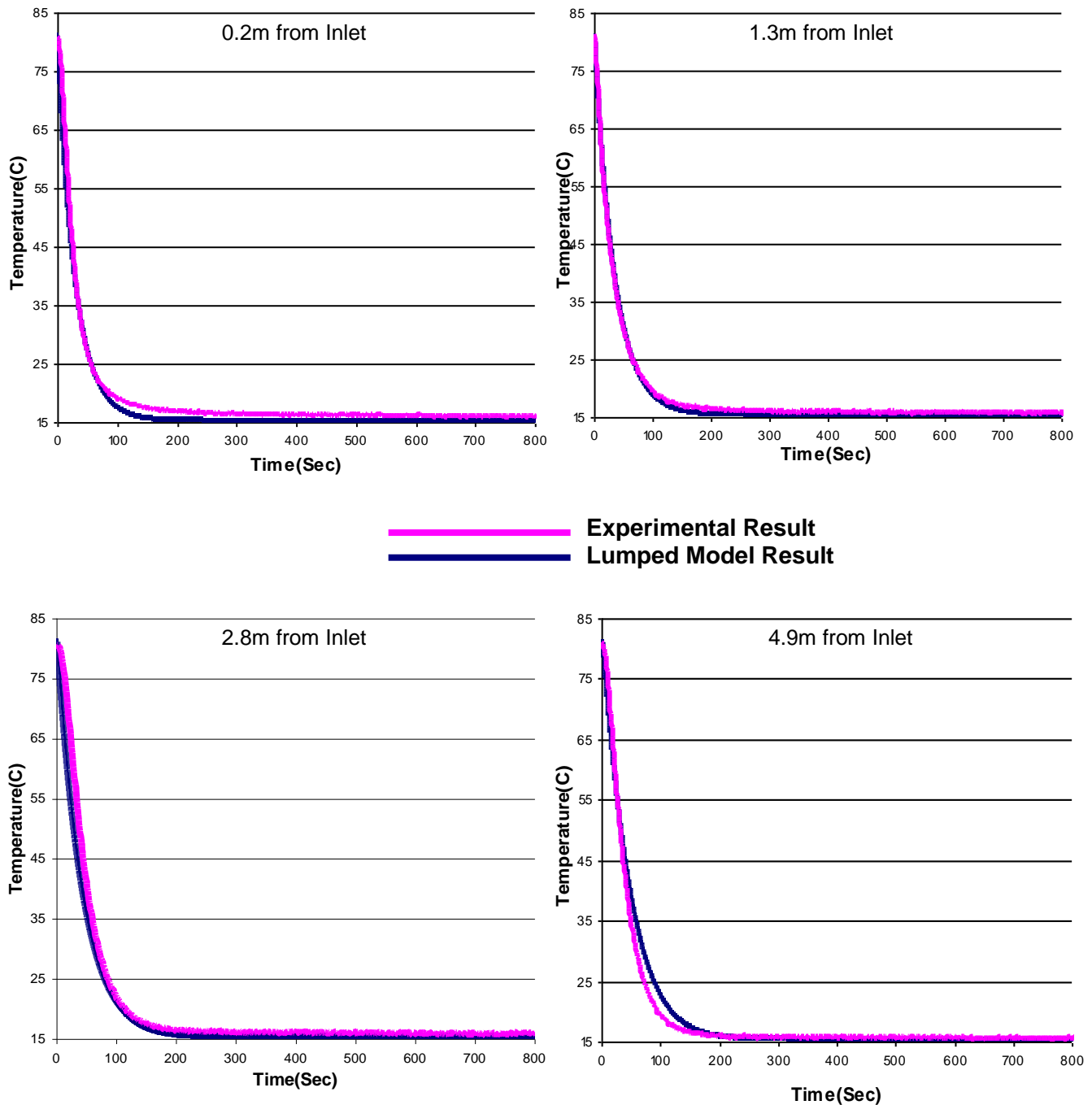
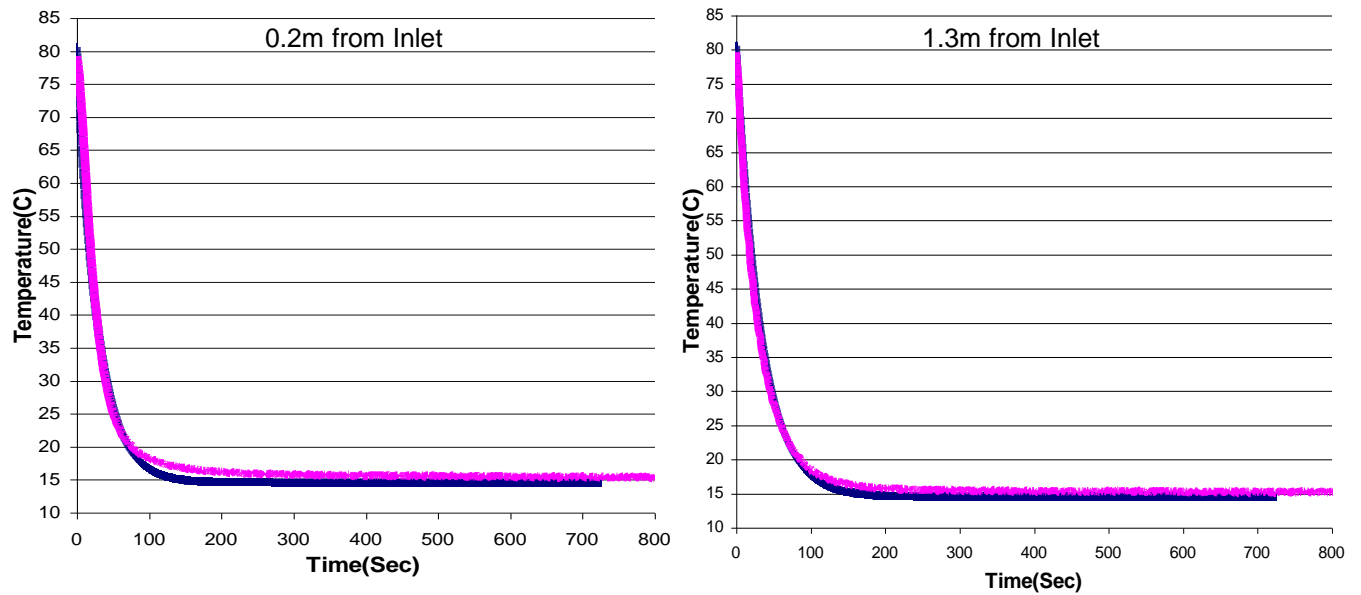


Figure 5.9: Comparisons between experimental and predicted cooling curves for 5.5 m long conductor cooled by 15.4°C water flowing through the cooling tube at a rate of 0.25 GPM. In all predictions, the radial heat resistance parameter (L^*) was chosen to be equal to 9 mm.

Conductor Length = 5.5 m, Water Flow Rate = 0.3 GPM
 Conductor Initial Temperature = 80.54°C, Water Inlet Temperature = 14.5°C



— Experimental Result
 — Lumped Model Result

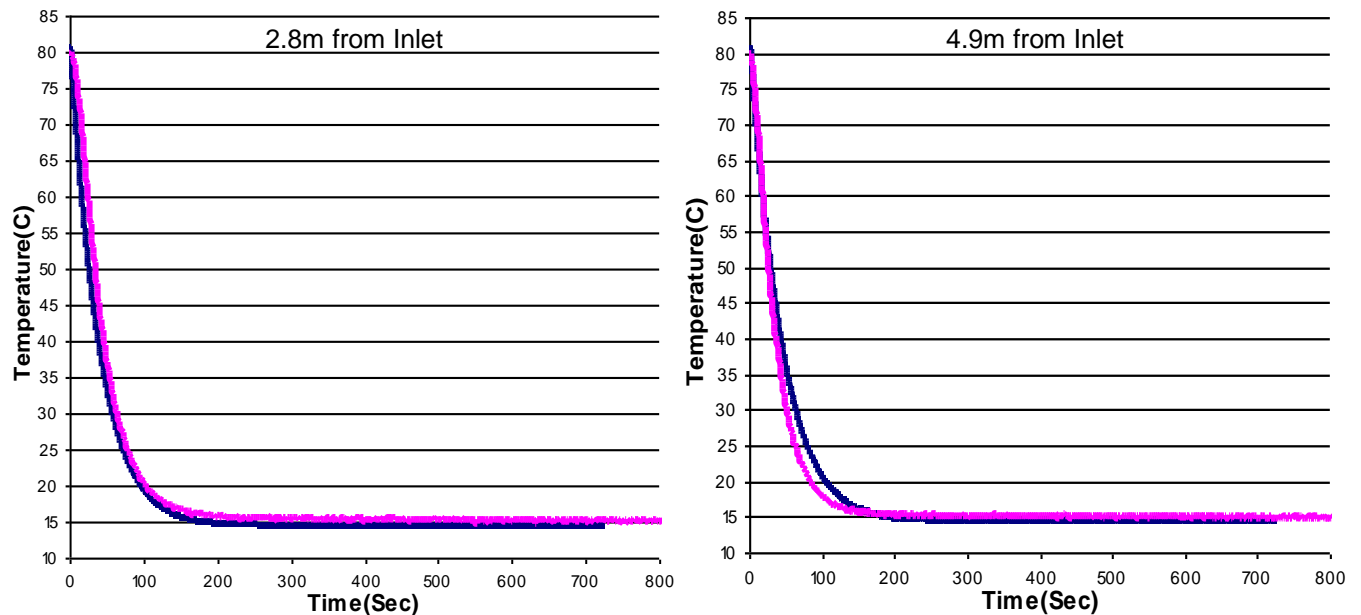
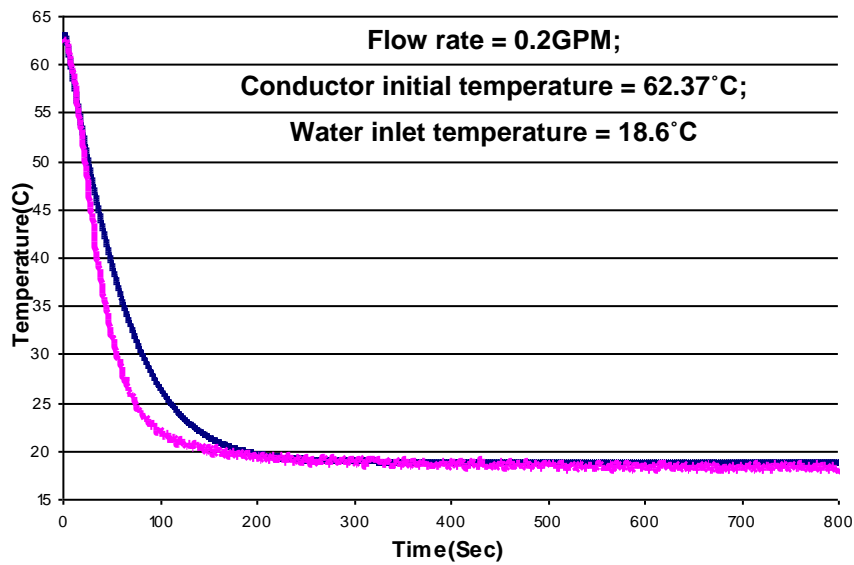
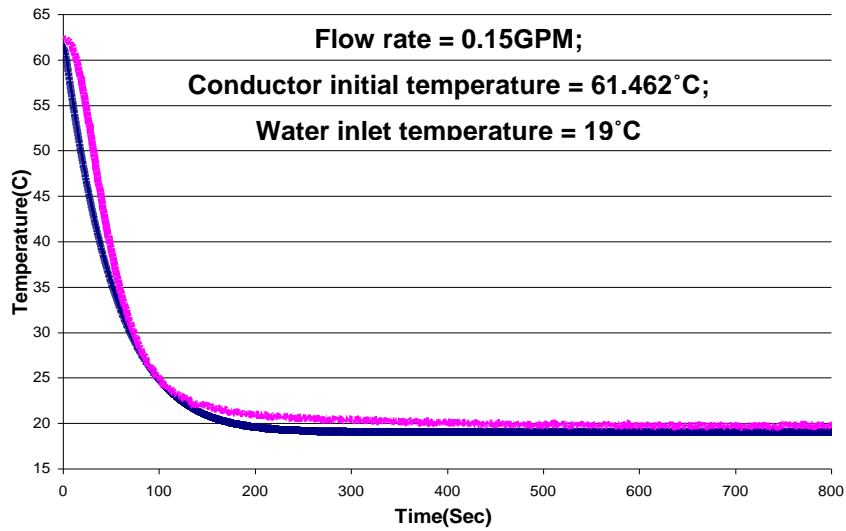
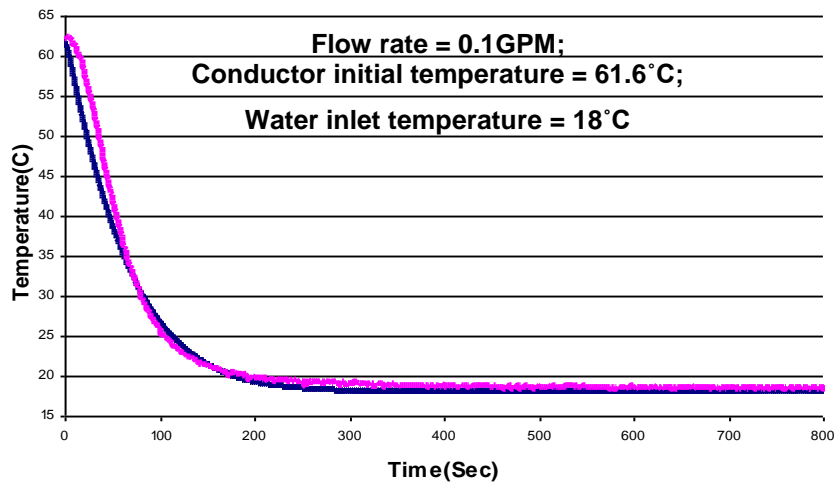


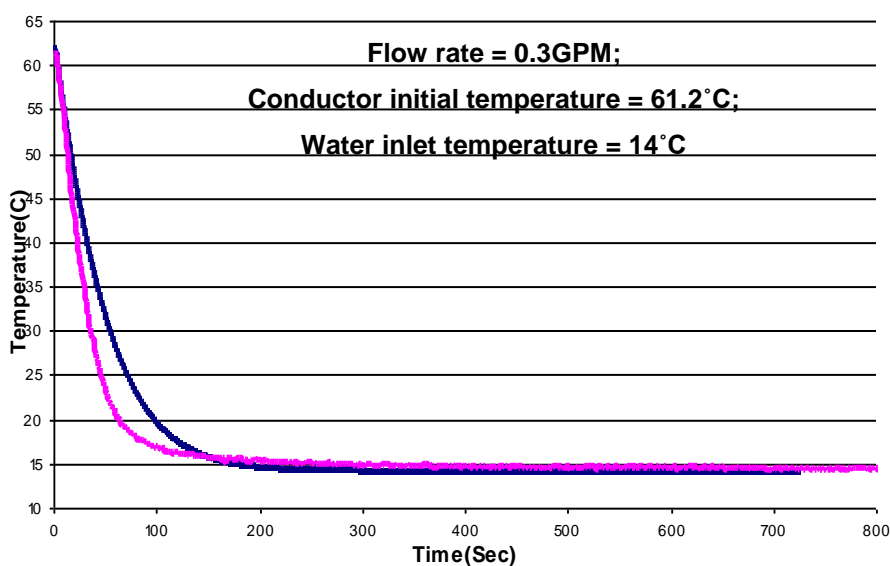
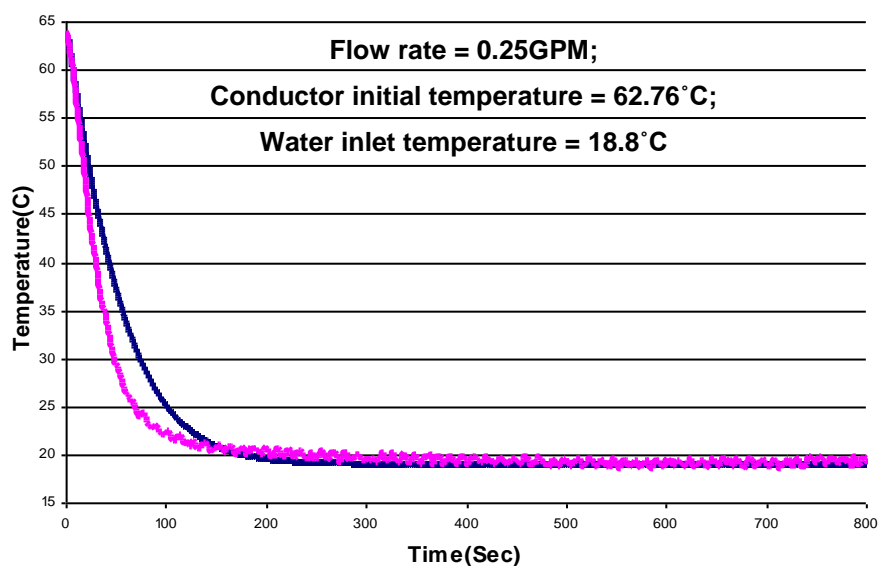
Figure 5.10: Comparisons between experimental and predicted cooling curves for 5.5 m long conductor cooled by 14.5°C water flowing through the cooling tube at a rate of 0.3 GPM. In all predictions, the radial heat resistance parameter (L') was chosen to be equal to 9 mm.

Exit Water Temperature



— Experimental Result — Lumped Model Result

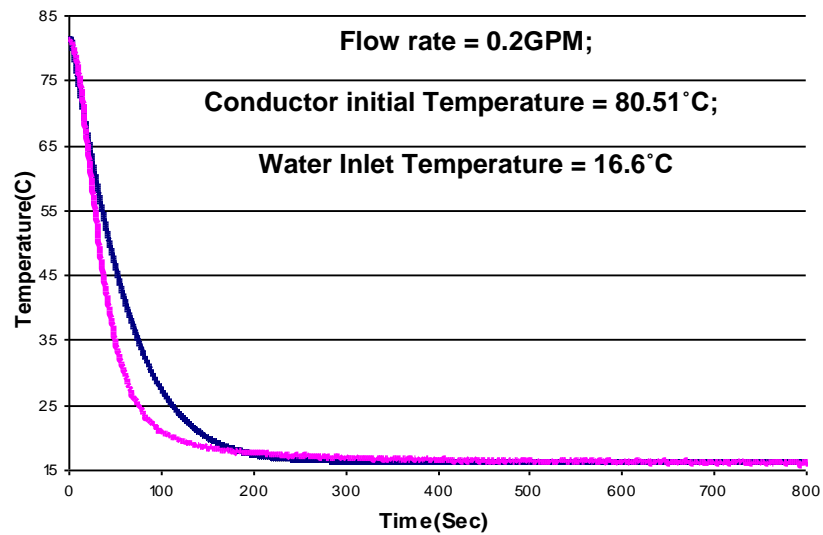
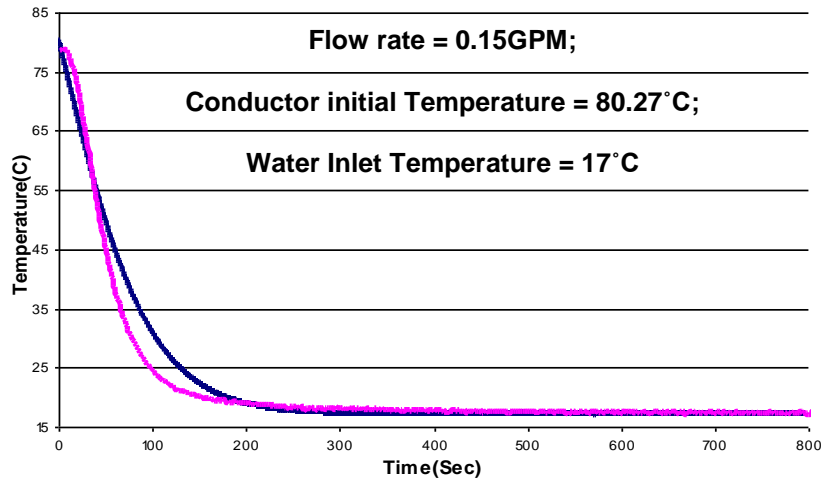
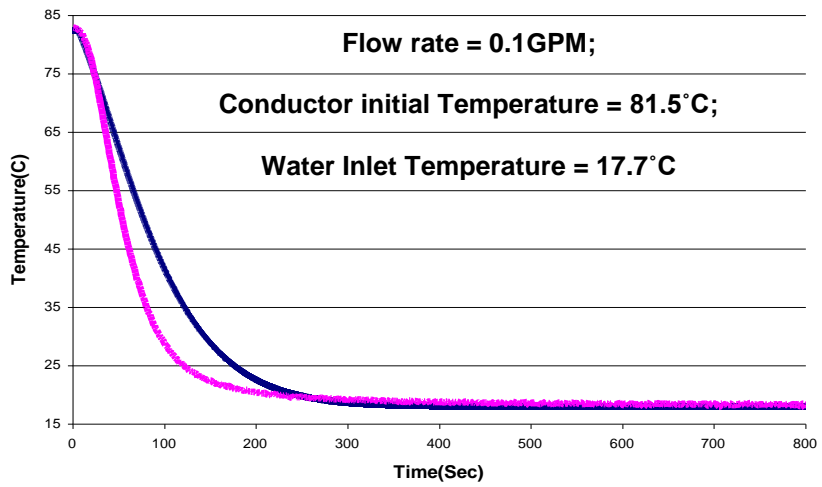
Exit Water Temperature



— Experimental Result — Lumped Model Result

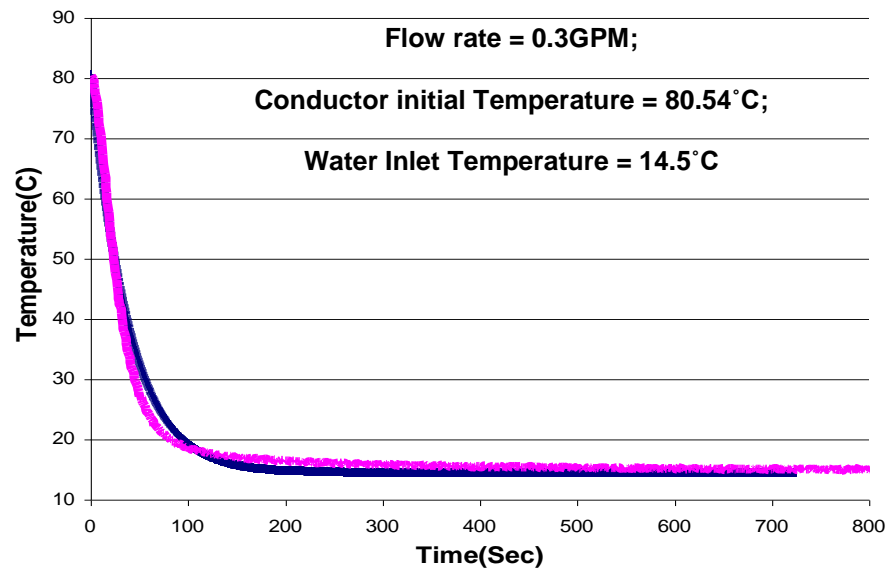
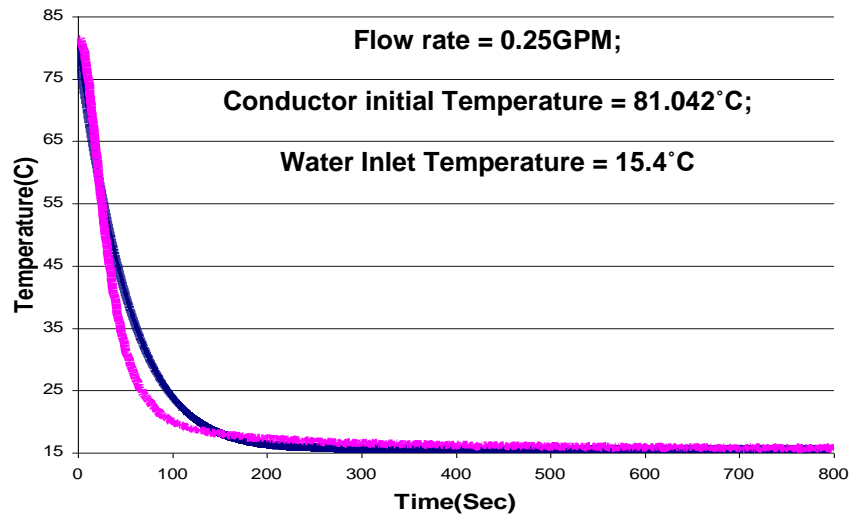
Figure 4.11: Comparisons between experimental and predicted exit water temperature versus time curves for 5.5 m long conductor that is cooled from its initial temperature of around 60°C by room temperature water flowing through the cooling tube at three different flow rates. In all predictions, the radial heat resistance parameter (L') was chosen to be equal to 9 mm.

Exit Water Temperature



— Experimental Result — Lumped Model Result

Exit Water Temperature



— Experimental Result — Lumped Model Result

Figure 5.12: Comparisons between experimental and predicted exit water temperature versus time curves for 5.5 m long conductor that is cooled from its initial temperature of around 80°C by room temperature water flowing through the cooling tube at three different flow rates. In all predictions, the radial heat resistance parameter (L) was chosen to be equal to 9 mm.

Following observations can be made from the figures:

- For all the flow rates, the Lumped Transient model together with the heat resistance parameter value of 9 mm maps the experimental data quite accurately for points located near the conductor inlet (i.e. 0.2 and 1.3 m from inlet, Figures 5.1 – 5.10) than those away from it. This was further validated quantitatively by calculating the correlation coefficient(r) between the experimental data and the predicted data for all the locations. Correlation coefficient is calculated for all the flow rates and temperatures and given in Table 5.2. The procedure for calculating r is explained in Appendix C. For all the cases, r value is positive and closer to +1 which means that there is a strong relationship between the experimental and predicted data. For the locations closer to the conductor (0.2m and 1.3m, Figures 5.1-5.10), r value is much closer to +1. However for the locations closer to the conductor end, the r values are lower.
- While the predicted and experimental cooling curves converge to the same temperature (inlet water temperature) in all cases, the predicted cooling rates were lower than those measured experimentally for points closer to conductor end (i.e. at points located at 2.3 and 4.8 m from inlet, Figures 5.1-5.10).
- The deviation between the predicted and experimental curves for points closer to conductor end decreases as the flow rate increases, Figures 5.1-5.10.

Table 5.2: Correlation Coefficient for all the flow rates

Conductor Temp	Flow Rate (GPM)	Distance From Inlet (m)	Correlation Coefficient (r)
≈60°C	0.1	0.2	0.996
		1.3	0.993
		2.8	0.986
		4.9	0.963
	0.15	0.2	0.998
		1.3	0.984
		2.8	0.970
		4.9	0.920
	0.2	0.2	0.993
		1.3	0.996
		2.8	0.980
		4.9	0.977
	0.25	0.2	0.995
		1.3	0.991
		2.8	0.979
		4.9	0.974
	0.3	0.2	0.997
		1.3	0.993
		2.8	0.989
		4.9	0.982

(Table 5.2 Continued)

Conductor Temp	Flow Rate (GPM)	Distance From Inlet (m)	Correlation Coefficient (r)
≈80°C	0.1	0.2	0.997616
		1.3	0.9939
		2.8	0.990252
		4.9	0.963846
	0.15	0.2	0.997651
		1.3	0.995107
		2.8	0.994777
		4.9	0.97964
	0.2	0.2	0.996521
		1.3	0.996064
		2.8	0.99396
		4.9	0.978583
	0.25	0.2	0.996432
		1.3	0.996669
		2.8	0.994408
		4.9	0.982314
	0.3	0.2	0.997115
		1.3	0.996056
		2.8	0.99367
		4.9	0.980811

Some of the possible sources that will explain the above noted observations are:

- The reason for lower cooling rate for locations closer to the conductor end as predicted by the lumped model may be due the neglect of axial heat transfer in the model. During the cooling process, there is also a temperature gradient along the length of the conductor with temperature rising as one travels from inlet to exit. Thus, considering that the axial thermal conductivity of the composite is much higher than its radial thermal conductivity (236 W/m.k in axial direction versus 9.9 W/m.k in radial direction [20]) the points near the conductor end are expected to lose some heat to elements towards the inlet due to the axial conduction as well. In the lumped model presented here the axial heat transfer between the adjacent composite elements was ignored. Only the radial heat conduction was modeled between the adjacent composite and water elements.
- Larger deviation between the predicted and experimental cooling curves for a flow rate of 0.1 GPM and for locations 2.3 and 4.8 m from inlet (Figures 5.1-5.10) can be due to the low Reynolds number at this flow rate. The Reynolds numbers are around 3500 at 0.1 GPM. At these values of Re , the flow can only be characterized as laminar or transitional. Whereas, at larger flow rates (0.2 GPM and higher), the flow is turbulent, which is what has been assumed in the model. The values of Reynolds numbers are given Table 5.3:

Table 5.3 – Reynolds numbers calculated in the model for different flow rates

Flow Rate (GPM)	Cond. Temp. (°C)	Water Temp. (°C)	Velocity	Reynold's Number	Nusselt Number	$\left(\frac{h_{\text{water}} W}{m^2 - k} \right)$	$\left(\frac{h_{\text{composite}} W}{m^2 - k} \right)$
0.1	61.6	18	0.77m/s	3474.413382	23.616143	4556.625091	949.853434
0.15	61.46	19	1.15m/s	5211.620072	36.781109	7096.744124	1026.43794
0.2	62.37	18.6	1.53m/s	6948.826763	48.915133	9437.947599	1064.63554
0.25	62.76	18.8	1.91m/s	8686.033454	60.401443	11654.17781	1087.97416
0.3	61.2	14	2.30m/s	10423.24014	71.426379	13781.38793	1103.88073
0.1	81.51	17.7	0.77m/s	3959.225400	26.063851	5028.898854	968.819492
0.15	80.27	17	1.15m/s	5938.838101	39.771844	7673.792414	1037.72439
0.2	80.51	16	1.53m/s	7918.450801	52.424586	10115.08021	1072.73620
0.25	81.042	15.4	1.91m/s	9898.063501	64.409007	12427.41860	1094.33068
0.3	80.54	14.5	2.30m/s	11877.67620	75.915011	14647.44859	1109.13363

- The third source for the difference in the predicted and experimental cooling curves may be attributed to the use of a same value of the radial heat resistance parameter, L^* for all cases. The radial temperature gradient, thus the centroid of the heat, does change somewhat with distance and time along the conductor; therefore, the L^* may not be a constant. A 10% increase in L^* using representative values of h and k , results in a change of approximately 8% in the value of B_i , i.e., the effect is of the same order as the change in L^* .

The comparison shown here demonstrates that the lumped transient model provides a simple engineering tool to predict the cooling time of internally cooled long conductors. A parametric analysis of this model can be used to determine the most optimum combination of the cooling parameters, such as flow rate, cooling medium (water, liquid nitrogen, etc.), cooling temperature, etc. to obtain the cooling of the conductor in a given amount of time. Such information is critical in the design of fusion reactors.

This lumped transient model with the same L^* value of 9 mm was used to predict the cooling behavior of 120 ft (36.5m) long QPS conductor embedded with copper tube. The predictions were made for two different cases: (a) when the conductor temperature is heated to 60 °C and cooled by water flowing at 0.1GPM at 18 °C, (b) when the conductor temperature is heated to 60 °C and cooled by water flowing at 0.2GPM at 18 °C. The results of these two cases are plotted below. In the figure 5.13, the 120 ft (36.5m) long conductor was heated to 60 °C and cooled by water flowing at 0.1GPM at 18 °C. The cooling profile for the five locations along the length of the conductor was plotted and the overall predicted cooling time for which the entire conductor cools down to Inlet water temperature is 1200 seconds.

Case (a):

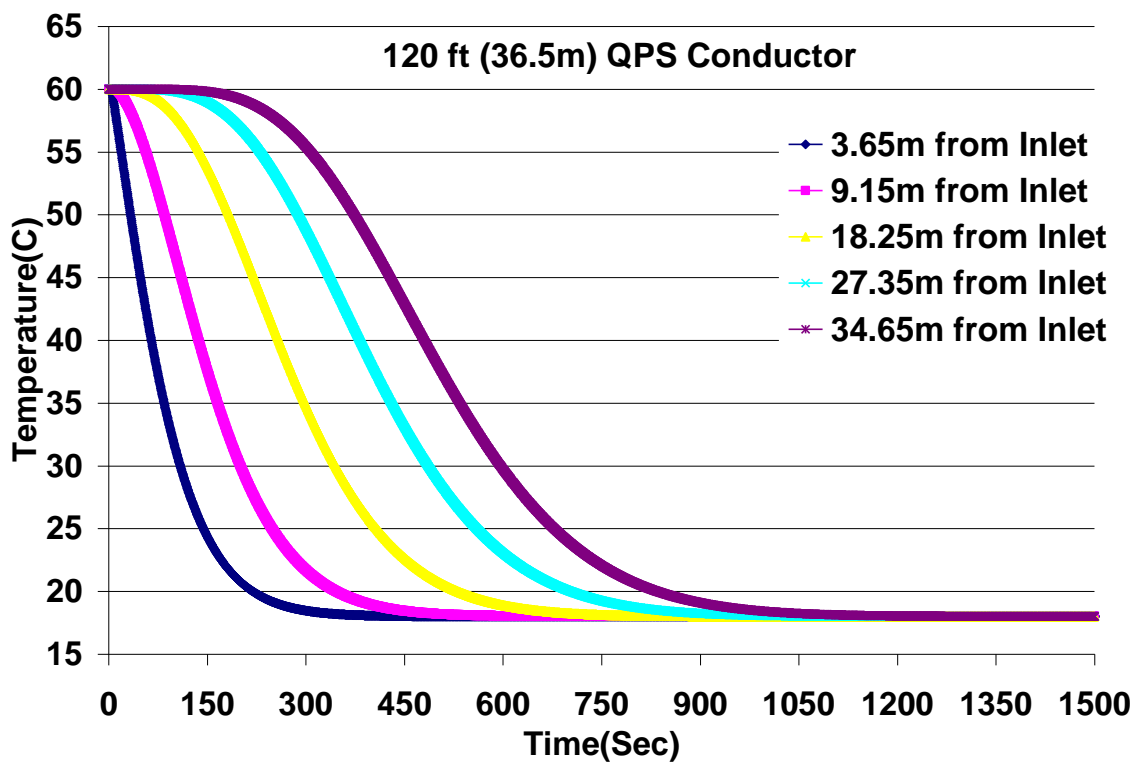


Figure 5.13: Predicted results for 120 ft (36.5m) long conductor heated to 60°C and cooled by 18°C water flowing through the cooling tube at a rate of 0.1 GPM. In all predictions, the radial heat resistance parameter (L^*) was chosen to be equal to 9 mm

Case (b):

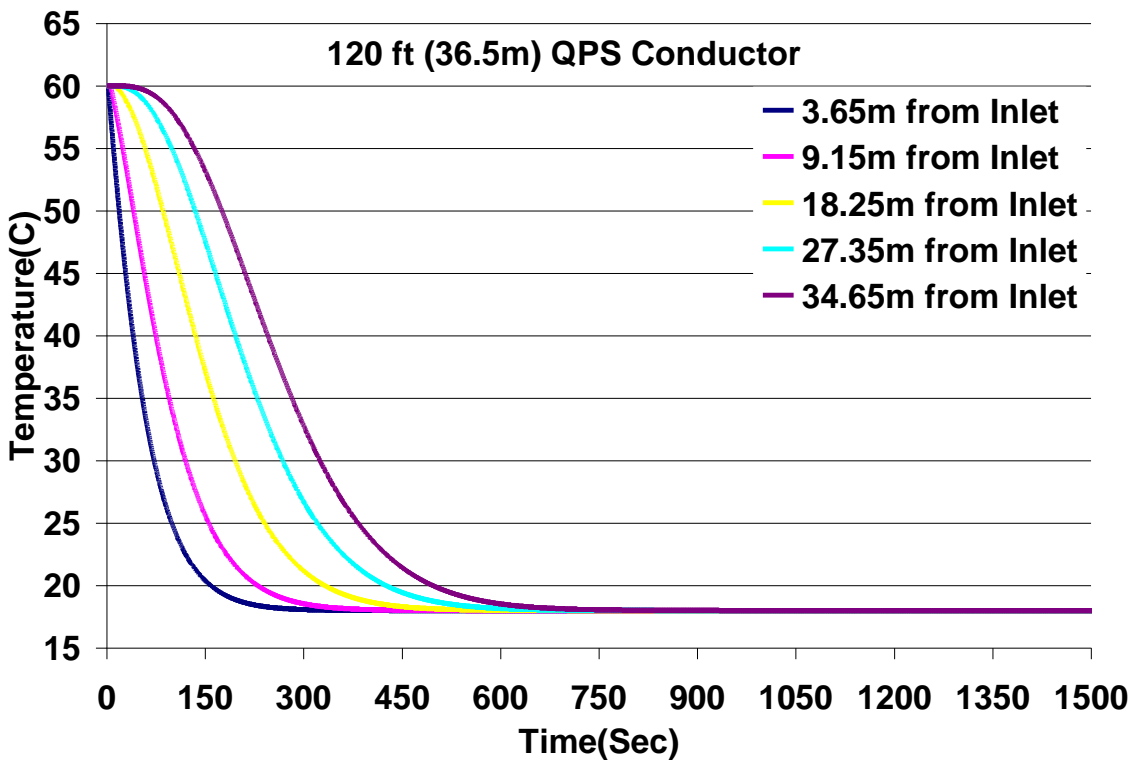


Figure 5.14: Predicted results for 120 ft (36.5m) long conductor heated to 60°C and cooled by 18°C water flowing through the cooling tube at a rate of 0.2 GPM. In all predictions, the radial heat resistance parameter (L') was chosen to be equal to 9 mm

In the above figure 5.14, the 120 ft (36.5m) long conductor was heated to 60 °C and cooled by water flowing at 0.2GPM at 18 °C. The cooling profile for the five locations along the length of the conductor was plotted and the overall predicted cooling time for which the entire conductor cools down to Inlet water temperature is 750 seconds. In comparison with the earlier Case (a), the predicted cooling time is lesser which means that as the flow rate increases the time taken for the conductor to cool down to Inlet water temperature decreases. This further validates the introduction of radial heat resistance parameter in the model and thus it can be used for predicting the cooling rate of 120 ft (36.5m) long QPS conductor for different temperatures and various flow rates.

6. CONCLUSIONS

This research was focused on: a) developing an experimental method to heat a long (5.5 m) stranded copper wire conductor containing an embedded copper cooling tube in the middle and then characterize the cooling behavior of the conductor by flowing water through the tube, b) developing a simple engineering tool to predict the cooling behavior of the same conductor, and c) comparing the predictions with experiments.

6.1 Experimental procedure for heating and cooling of 5.5m (~18ft) QPS conductor:

Two heating methods – heat tape and forced air convection oven - were used to heat the conductor. After several attempts with both methods, the forced air convection was adopted for all experiments. After several iterations, an experimental method was developed that produced uniform heating and cooling of the conductor and reproducible data. The following conclusions were reached in this regard: A two-way flow control valve added to ensure that the cooling water temperature did not change during the exp The results were reproducible and for performing the experiments on the conductor for heating and cooling after analyzing the results of various iterations.

- Heating Uniformity: There was a significant variation in the temperature recorded by the different thermocouples when the conductor was heated using heat tape. It was difficult to manually control the temperature of individual thermocouples in heat tape heating. This was because the thermocouples that were closer to the heat tape were heated faster than those away from it. Heating the conductor using the Forced air convection oven led to uniform heating of the entire conductor. The temperatures of all thermocouples reached the same preset temperature with temperature variations among different thermocouples less than 1°C.
- Cooling Uniformity: Even though all the thermocouples converged to the desired temperature using forced air convection heating, there were issues with cooling the conductor. It was found that the temperature of the water entering at the inlet was varying during the experiment. An addition of a two-way flow control valve before the inlet solved this problem.

6.2 Heat transfer analysis of the conductor using the elemental approach:

- An elemental approach was developed in MATLAB© software using the Lumped transient analysis.
- Experimental data collected was used to verify the results of this elemental approach so that this approach can be used in predicting the cooling time of long QPS conductors.
- A radial heat resistance parameter was introduced in the lumped model and it was calculated empirically. This was done by fitting the data for a set of flow rate-temperature-location. The same value was used to predict cooling rates for all other flow rates, temperatures and locations.
- The introduction of this radial heat resistance parameter resolved certain issues the Biot number discrepancy. The predicted cooling curves agreed quite well with the experimental curves for the location near the inlet. However, for the conductor points near the exit end, the model predicted slower cooling rate than measured experimentally. Recommendations are made to further modify the model that may improve its predictability.

The main objective of this research was to predict the cooling time of a long QPS conductor when cooled by water flowing under different conditions through the middle tube. While the predicted cooling curves may not match exactly the experimental curves for all cases, the predicted cooling time (the time it takes the conductor to cool from high temperature to within one degree Celsius of the inlet water temperature) is close to that measured experimentally. Also noteworthy is that the modeling approach used here is simple to implement and can be used as an engineering tool to study the effect of thermal and flow variables on the total cooling time of long conductors. Such information is crucial for the design of QPS conductors.

7. FUTURE WORK

7.1 Elemental Approach (Lumped Transient Model)

- The model presented here did not include axial heat transfer. Considering that the axial thermal conductivity of composite is much larger compared to its radial thermal conductivity (230W/m.k in axial direction versus 9.9 W/m.k in radial direction), there may be some redistribution of heat due to axial heat transfer.
- The use of a same value of the radial heat transfer parameter ($L^* = 9 \text{ mm}$) may not be justified. Since the L^* relates to the temperature gradient in the conductor, it must vary with location along the conductor length as well as with flow and thermal conditions. Thus, it is recommended that a new value of L^* should be found for each case.
- The predictions should be verified for other sets of experimental data such as conductors with different cross-sections and lengths.

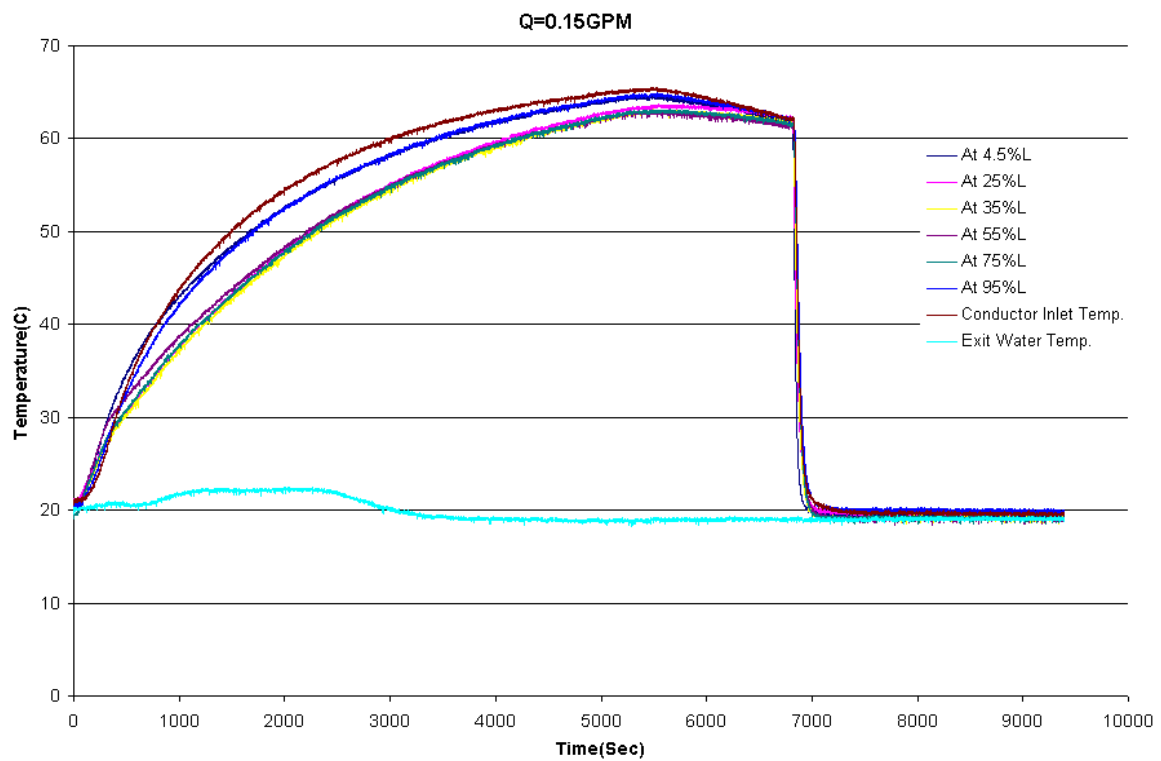
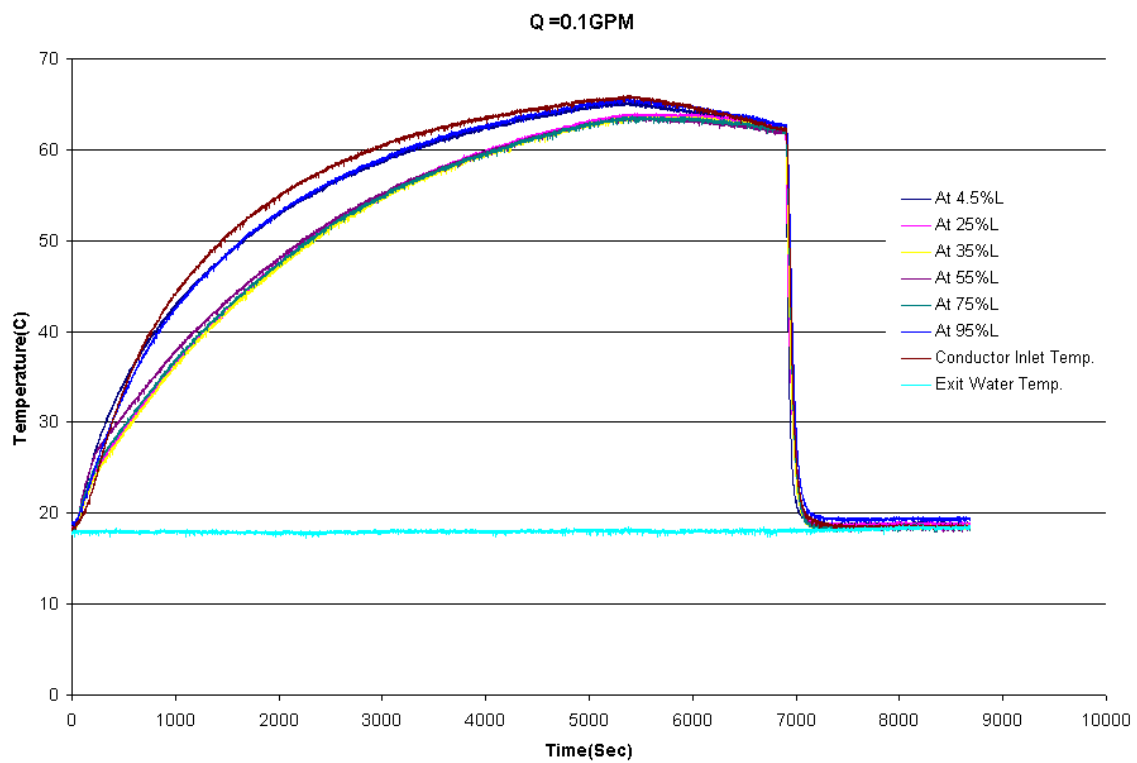
REFERENCES

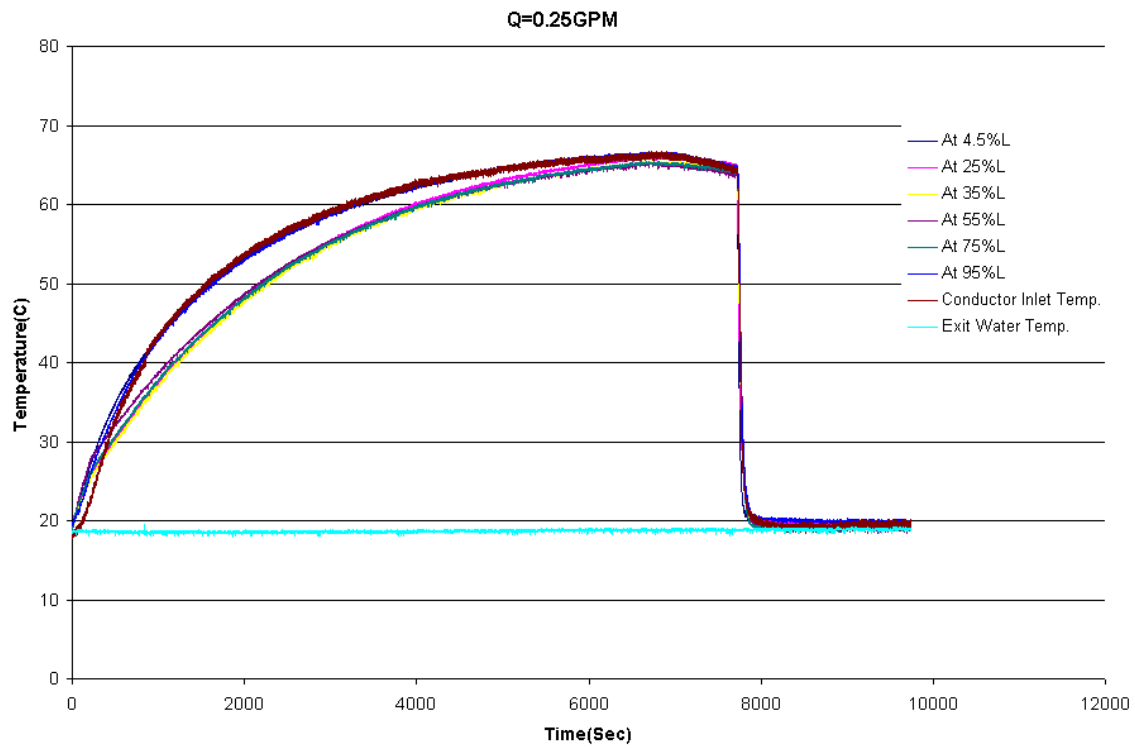
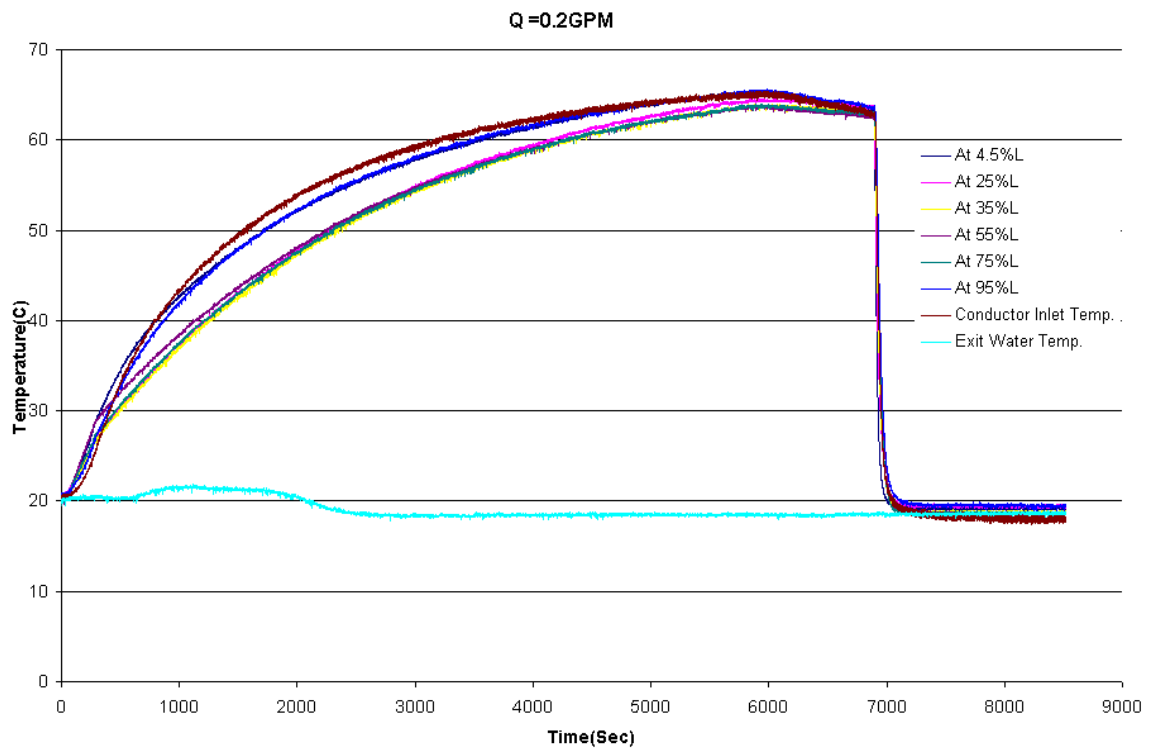
1. B. E. Nelson, R.D. Benson, P.J. Fogarty, P.L. Goranson, Design of Quasi Poloidal Stellarator Experiment (QPS), *Fusion Engineering and Design* (2003) 205-210.
2. K.D. Freudenberg, P. Goranson and F. Dahlgren, Cooling design and analysis of the QPS modular coil winding packs, 21st IEEE/NPSS Symposium On Fusion Engineering, (2005).
3. A. Chaudhri, Thermal Modeling and Verification of a Quasi-Poloidal Stellarator Modular Coil. MS Thesis, August (2004), The University of Tennessee, Knoxville.
4. C.W. Leung and S. D. Probert, Applied Energy, **50**, 313 (1995).
5. C.W. Leung and S. D. Probert, Applied Energy, **57**, 13 (1997).
6. G. Wang and S.P. Vanka, International Journal of Heat and Mass Transfer, **38**, 3219 (1995).
7. Yauo Mori and Wataru Nakayama, International Journal of Heat and Mass Transfer, **10**, 1801-1813 (1967).
8. X. Lu, P. Tervola, M. Viljanen, International Journal of Heat and Mass Transfer, **49**, 341 (2006).
9. X. Lu, P. Tervola, M. Viljanen, International Journal of Heat and Mass Transfer, **49**, 1107 (2006).
10. E.K. Kalinin and G.A. Dreitser, International Journal of Heat and Mass Transfer, **28**, 361 (1985).
11. Yuzhi Sun and Indrek S. Wichman, International Journal of Heat and Mass Transfer, **47**, 1555 (2004).
12. F. de. Monte, Transient Heat Conduction in One-Dimensional Composite Slab. A 'Natural' Analytic Approach. *Int. J. Heat Mass Transfer* **43** (19) (2000) 3607–3619.
13. F. de Monte, An Analytic Approach to the Unsteady Heat Conduction Processes in One-Dimensional Composite Media. *Int. J. Heat Mass Transfer* **45**, (2002) 1333-1343.
14. Abram Dorfman, Journal of Heat Transfer, **126**, 149 (2004)
15. J. P. Holman, *Heat Transfer*, 6th Edition. Unsteady-State Conduction, pp. 131-135 (1986) McGraw-Hill.
16. P. L. Goranson, B. Nelson, J. Ping, Design of the Plasma Facing Components for the National Spherical Tokamak Experiment (NSTX). 18th IEEE/NPSS Symposium on Fusion Engineering, Albuquerque, New Mexico, p. 67, Oct. 25-29 (1999).
17. S. Narasimhaswami, Cooling of QPS Modular Coils Using Embedded Copper Tubes. MS Thesis, December (2006), University of Tennessee, Knoxville.

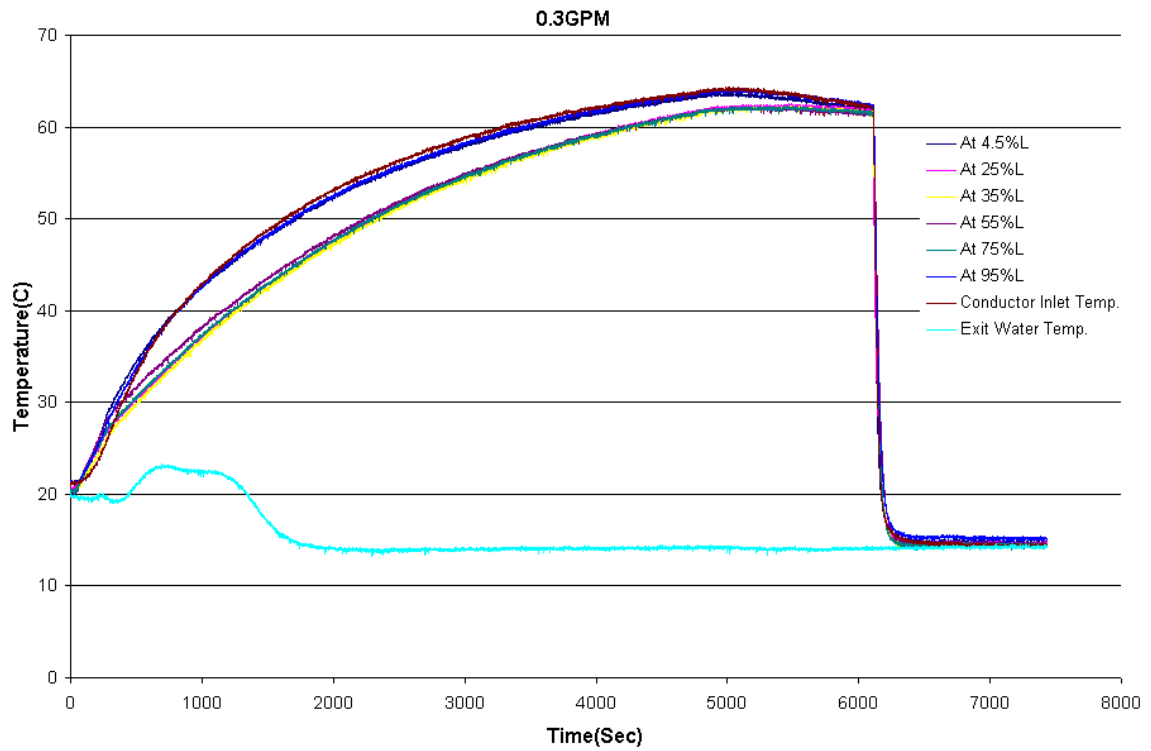
18. V. Gnielinski, New Equations for Heat and Mass Transfer in Turbulent Pipe Channel Flow, Int. Chem. Eng., Vol. 16, (1976) pp. 359-368.
19. V. Gnielinski, Single Phase Convective Heat Transfer. Ch. 2.5, sections 1 – 2. (1983) Hemisphere Publishing Corporation. Eng.
20. B. S. Petukhov, , Heat Transfer and Friction in Turbulent Pipe Flow with Variable Physical Properties. Advances in Heat Transfer. In: Irvine, T.F. and Hartnett, J.P. (eds.), Vol. 6, (1970) Academic Press, New York. pp. 503-565.
21. Chin-Chi Tsai, B. E. Nelson, H. Wang, Thermal Diffusivity Measurements of Monolithic Copper-Epoxy Composite Specimens by the Flash Method. 27th International Thermal Conductivity Conference (ITCC27) and the 15th International Thermal Expansion Symposium (ITES15), Ed. H. Wang and W.D. Porter, (2006) pp, 413-423.
22. <http://www.socialresearchmethods.net/kb/statcorr.php>
23. <http://web.utk.edu/~qps>

Appendices

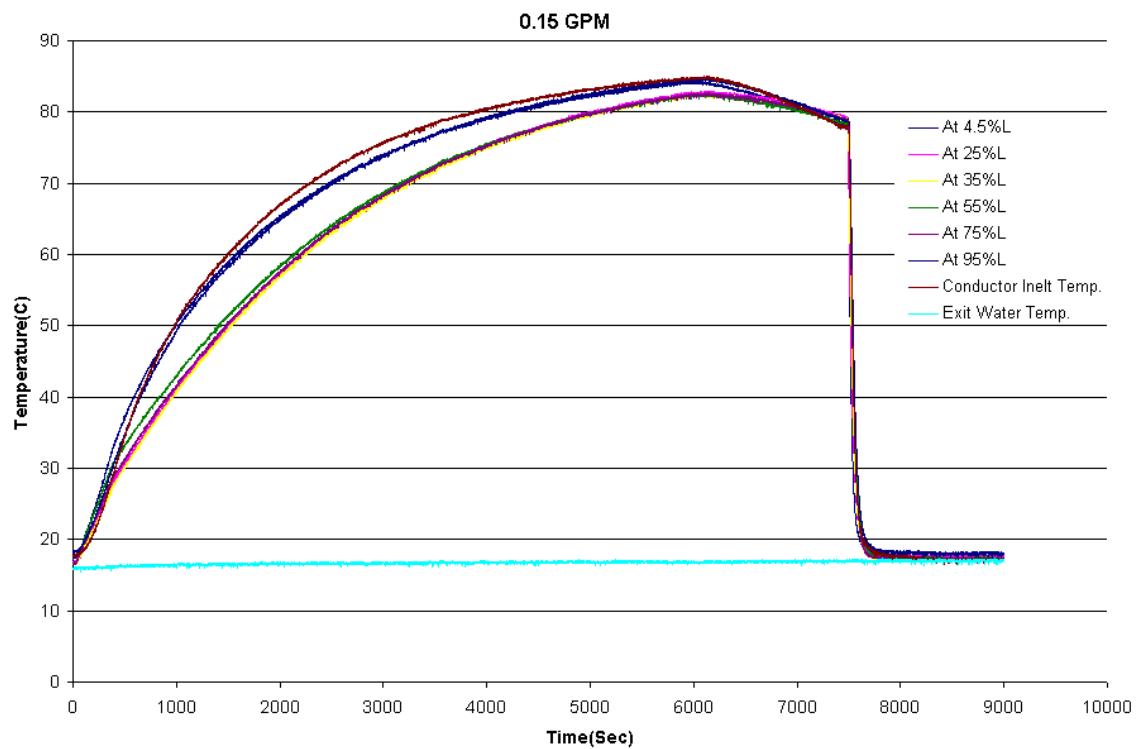
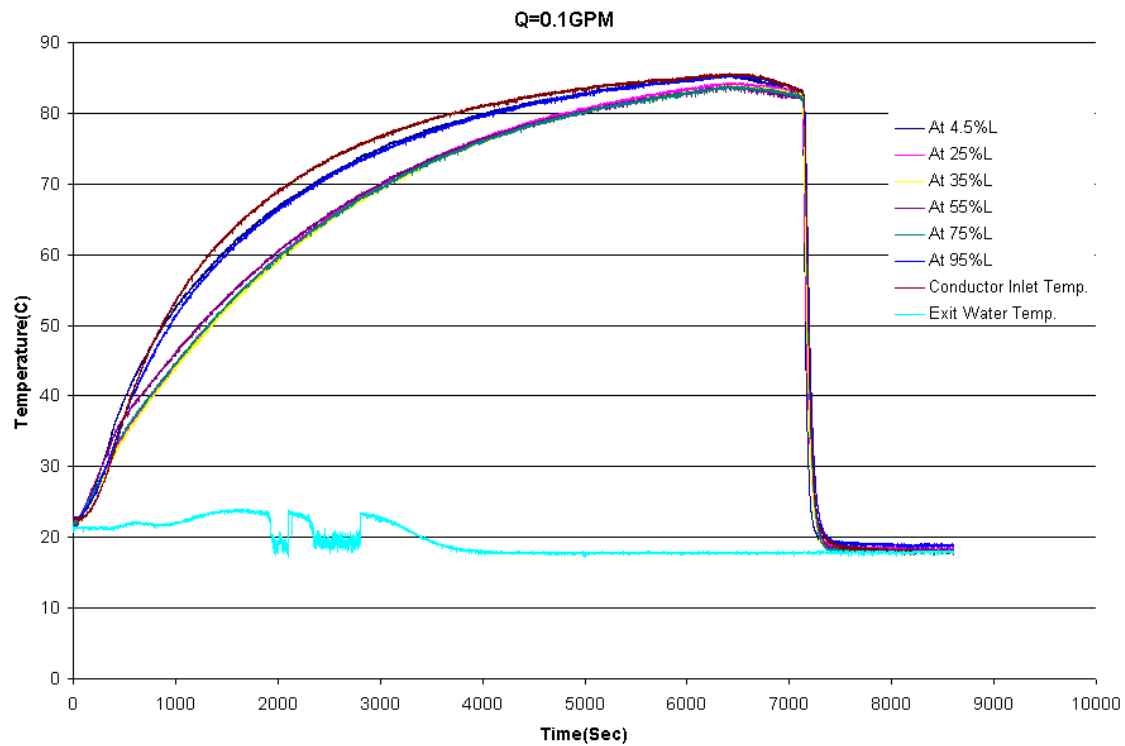
Appendix A

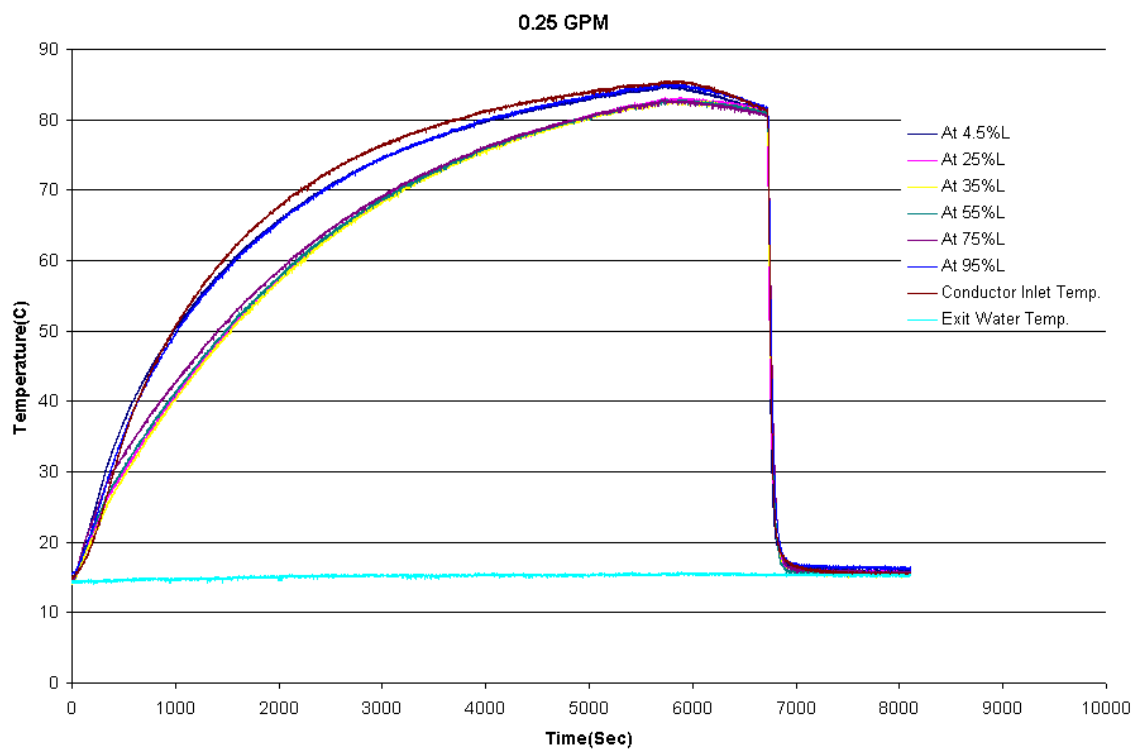
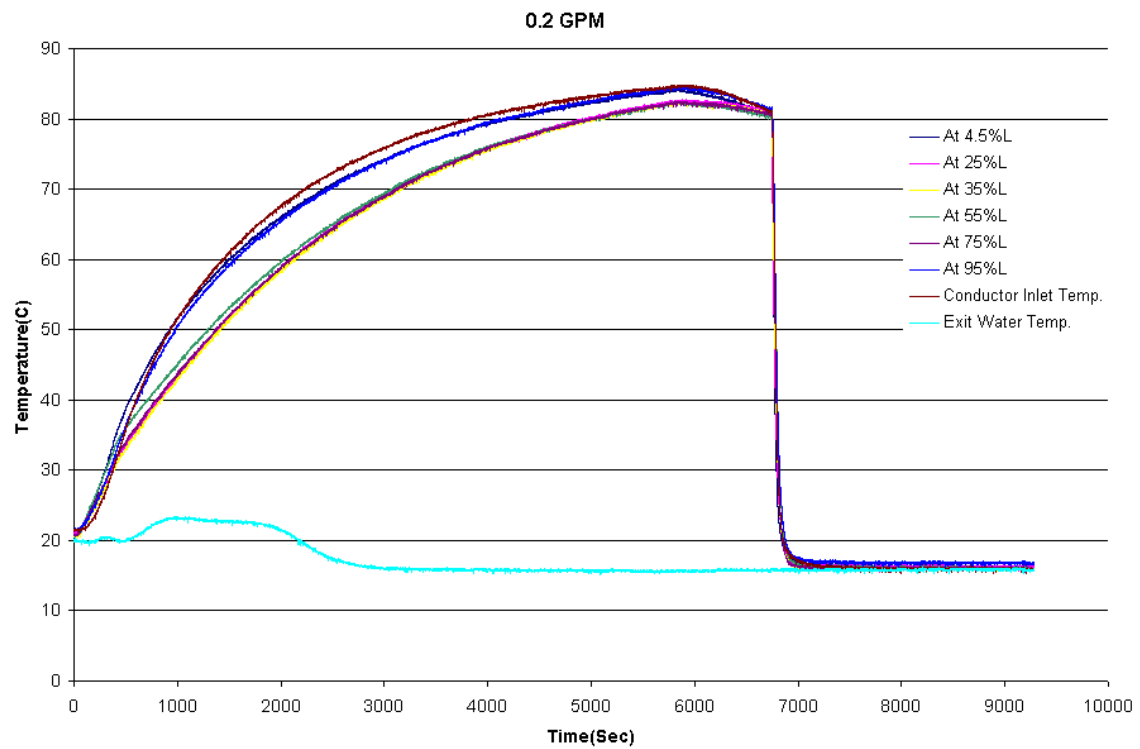


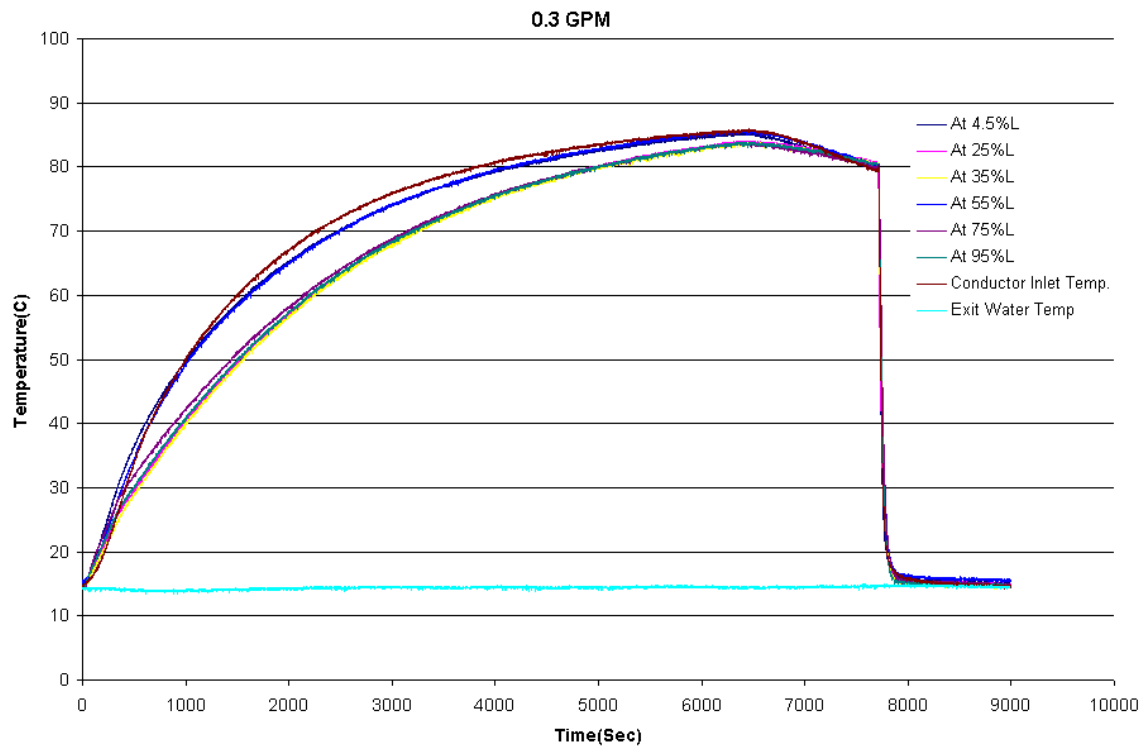




All Experimental results for 5.5 m long conductor when heated to around $\approx 60^{\circ}\text{C}$ with five different water flow rates(0.1GPM,15GPM, 0.2GPM, 0,25GPM, 0.3GPM) flowing through the cooling tube.







All Experimental results for 5.5 m long conductor when heated to around $\approx 80^{\circ}\text{C}$ with five different water flow rates(0.1GPM,15GPM, 0.2GPM, 0,25GPM, 0.3GPM) flowing through the cooling tube.

Appendix B

```

% HEAT TRANSFER ANALYSIS OF QPS COIL

clc
clear all
% Lumped system analysis
% All units in SI system

% ---- User defined variables ----
Q=0.1; %in gal/min
ri = 0.003239/2; %inside radius in m
A=(pi)*(ri^2); % Cross sectional area in m^2
v= (0.003785412)*(Q)/((A)*(60));% Velocity of water in m/s
length_of_tube = 5.5 ; % in m
time_of_result = 1000; % result wanted at end of this time period.
n = 1000; % number of elements in the model

Excel = actxserver('Excel. Application');
    set(Excel, 'Visible', 1);
    % Insert a new workbook
    Workbooks = Excel.Workbooks;
    Workbook = invoke(Workbooks, 'Add');

start_time = cputime ;
% calculation of time step for the given no. of elements
    t_inlet_to_outlet = length_of_tube/v ;
    t = t_inlet_to_outlet/n ;

% ---- User Print screen data ----
    sprintf ('Length of tube considered = %.2f m.',length_of_tube)
    sprintf ('Velocity of water = %.2f m/s',v)
    sprintf ('Temperature distribution required at time = %.3f seconds', time_of_result)
    sprintf ('Number of elements used in the model = %.0f ',n)
    sprintf ('Time step used in the model = %.8f ',t)

% ---- Property Values -----

```



```

k = 9.9; % Conductivity of Composite 12 W/m-K
Tcomposite = 61.6; % Initial temp of Cu composite -- provided later as Tc
Twater_inlet = 18; % Initial temp of water -- provided later as Tw
rho_cyanate_ester = 1300 ; %Kg/m3
rho_Cu = 8933; %Kg/m3 Earlier value 8940
vol_fraction_Cu = 0.78;

% Density of composite from volume fraction
rho = (vol_fraction_Cu * rho_Cu) + ( (1-vol_fraction_Cu)*rho_cyanate_ester );
Cp_epoxy = 865;% Specific heat of epoxy in SI J/kg-K
Cp_cu = 385; % Specific heat of Copper in SI J/kg-K
Cp = (vol_fraction_Cu * Cp_cu) + ( (1-vol_fraction_Cu)*Cp_epoxy );
rho_w = 1000; %density of water
Cpw = 4200; %Specific heat of water

% -----Geometry of tube -----
ro = 0.005643326;% Outside radius in m
ri = 0.003239/2; %inside radius in m
%display ('Effective surface length L is :')
L= (ro^2 - ri^2) / (2*ri) ;% Effective length calculated from Volume / Surface Area
%display ('Fourier number Fo is :')
Fo = k/(rho*Cp) * t/L^2;
vwater=7.13805/10^7; % Kinematic Viscosity of water
Prwater=4.793; % Prandtl Number of water
Re= (v)*(2*ri)/(vwater); %Reynolds number
f = 1/((0.790*log(Re))-1.64)^2; % Darcy frictional factor
Nu = ((f/8)*(Re-1000)*Prwater)/ (1+ (12.7*(f/8)^(1/2)*(Prwater^(2/3)-1)));
kwater=0.62495; %Thermal conductivity of water
hwater= (Nu)*(kwater)/(2*ri); %Convective heat transfer coefficient of water
hinverse=(1/hwater)+(0.009/k);%Inverse of the resistance term
h=(1/hinverse);%Resistance term
Bi= (h*L)/k; %Conductivity of composite.
sprintf('Reynolds number = %.6f',Re)
sprintf('Darcy friction factor = %.6f',f)
sprintf('Nusselt number= %.6f',Nu)
sprintf ('Biot Number = %.8f',Bi)
mass_element_w = pi *(ri^2) * (length_of_tube/n) * rho_w ;

```

```

mass_entire_composite = pi * (ro^2 - ri^2) * length_of_tube * rho ;
mass_each_element_composite = mass_entire_composite / n;

total_heat_lost_composite = mass_entire_composite * Cp * (Tcomposite - Twater_inlet);

Tc(1:n)=Tcomposite; % initial temperature of composite in C
Tw(1:n) = Tcomposite;
Sum_of_DeltaT = 0 ;
count = 1;
temp=1;
DeltaT = 0;

%fprintf('Beginning of the first loop')
for time=t:t:time_of_result

    for i=1:n

        Tcafter(i) = ((Tc(i)-Tw(i)) * exp(-Bi*Fo)) + Tw(i);
        Twafter(i) = Tw(i) + ( (ro^2-ri^2)*rho*Cp*( Tc(i)-Tcafter(i)))/(ri^2*rho_w*Cpw);

    end

    %fprintf('end of the second loop',time)
    T_mid45_element_Cu(count)=Tcafter(0.045*n);
    T_mid250_element_Cu(count)=Tcafter(.25*n);
    T_mid350_element_Cu(count)=Tcafter(.35*n);
    T_mid450_element_Cu(count)=Tcafter(.45*n);
    T_mid550_element_Cu(count)=Tcafter(.55*n);
    T_mid650_element_Cu(count)=Tcafter(.65*n);
    T_mid750_element_Cu(count)=Tcafter(.75*n);
    T_mid950_element_Cu(count)=Tcafter(.95*n);
    T_outlet_element_water(count)=Twafter(n);

    Tc = Tcafter;
    Twintermediate = Twafter;
    Twintermediate = Twintermediate( 1:(n-1) );

```

```

Twnew=[Twater_inlet,Twintermediate];
Tw=Twnew;

time_steps(count)=time;
T_bulk_Cu(count) = sum(Tcafter(980:n))/20 ;
T_bulk_w(count) = sum(Twafter(980:20))/20;
count = count + 1;
end

if time_of_result - time > 0
    sprintf('Temperature distribution was calculated at %.3f seconds.\nTemperature distribution
was requested at %.3f seconds.\nTo calculate at the exact time, please increase the number of
elements.',time,time_of_result)
end

time_steps_excel = time_steps(1:10:end);
T_mid45_element_Cu_excel=T_mid45_element_Cu(1:10:end);
T_mid250_element_Cu_excel=T_mid250_element_Cu(1:10:end);
T_mid350_element_Cu_excel=T_mid350_element_Cu(1:10:end);
T_mid450_element_Cu_excel=T_mid450_element_Cu(1:10:end);
T_mid550_element_Cu_excel=T_mid550_element_Cu(1:10:end);
T_mid650_element_Cu_excel=T_mid650_element_Cu(1:10:end);
T_mid750_element_Cu_excel=T_mid750_element_Cu(1:10:end);
T_mid950_element_Cu_excel=T_mid950_element_Cu(1:10:end);
T_outlet_element_water_excel=T_outlet_element_water(1:10:end);
T_bulk_Cu_excel=T_bulk_Cu(1:10:end);
T_bulk_w_excel=T_bulk_w(1:10:end);

% Make the second sheet active
Sheets = Excel.ActiveWorkBook.Sheets;
sheet_v = get(Sheets, 'Item', 1);
invoke(sheet_v, 'Activate');

% Get a handle to the active sheet
Activesheet = Excel.Activesheet;

% Put a MATLAB array into Excel
ActivesheetRange = get(Activesheet,'Range','A2');
set(ActivesheetRange, 'Value', 'time steps(s)');
ActivesheetRange = get(Activesheet,'Range','A3:A65000');

```

```
set(ActivsheetRange, 'Value', time_steps_excel(:));
```

```
ActivsheetRange = get(Activsheet,'Range','B2');  
set(ActivsheetRange, 'Value', 'Cu 4.5%L Temp.(C)');  
ActivsheetRange = get(Activsheet,'Range','B3:B65000');  
set(ActivsheetRange, 'Value', T_mid45_element_Cu_excel(:));
```

```
ActivsheetRange = get(Activsheet,'Range','C2');  
set(ActivsheetRange, 'Value', 'Cu 25%L Temp.(C)');  
ActivsheetRange = get(Activsheet,'Range','C3:C65000');  
set(ActivsheetRange, 'Value', T_mid250_element_Cu_excel(:));
```

```
ActivsheetRange = get(Activsheet,'Range','D2');  
set(ActivsheetRange, 'Value', 'Cu 35%L Temp.(C)');  
ActivsheetRange = get(Activsheet,'Range','D3:D65000');  
set(ActivsheetRange, 'Value', T_mid350_element_Cu_excel(:));
```

```
ActivsheetRange = get(Activsheet,'Range','E2');  
set(ActivsheetRange, 'Value', 'Cu 45%L Temp.(C)');  
ActivsheetRange = get(Activsheet,'Range','E3:E65000');  
set(ActivsheetRange, 'Value', T_mid450_element_Cu_excel(:));
```

```
ActivsheetRange = get(Activsheet,'Range','G2');  
set(ActivsheetRange, 'Value', 'Cu 65%L Temp.(C)');  
ActivsheetRange = get(Activsheet,'Range','G3:G44780');  
set(ActivsheetRange, 'Value', T_mid650_element_Cu_excel(:));
```

```
ActivsheetRange = get(Activsheet,'Range','H2');  
set(ActivsheetRange, 'Value', 'Cu 75%L Temp.(C)');  
ActivsheetRange = get(Activsheet,'Range','H3:H44780');  
set(ActivsheetRange, 'Value', T_mid750_element_Cu_excel(:));
```

```
ActivsheetRange = get(Activsheet,'Range','I2');  
set(ActivsheetRange, 'Value', 'Cu 95%L Temp.(C)');  
ActivsheetRange = get(Activsheet,'Range','I3:I65000');  
set(ActivsheetRange, 'Value', T_mid950_element_Cu_excel(:));
```

```
ActivsheetRange = get(Activsheet,'Range','J2');  
set(ActivsheetRange, 'Value', 'Water exit Temp.(C)');  
ActivsheetRange = get(Activsheet,'Range','J3:J65000');  
set(ActivsheetRange, 'Value', T_outlet_element_water_excel(:));
```

```
ActivsheetRange = get(Activsheet,'Range','K2');  
set(ActivsheetRange, 'Value', 'Cu Temp. along length(C)');  
ActivsheetRange = get(Activsheet,'Range','K3:K65000');  
set(ActivsheetRange, 'Value', Tcafter(:));
```

```
ActivsheetRange = get(Activsheet,'Range','L2');
```

```

set(ActivsheetRange, 'Value', 'Water Temp. along length(C)');
ActivsheetRange = get(Activsheet,'Range','L3:L65000');
set(ActivsheetRange, 'Value', Twafter(:));

```

```

ActivsheetRange = get(Activsheet,'Range','M2');
set(ActivsheetRange, 'Value', 'Cu bulk Temp. with time(C) ');
ActivsheetRange = get(Activsheet,'Range','M3:M65000');
set(ActivsheetRange, 'Value', T_bulk_Cu_excel(:));

```

```

ActivsheetRange = get(Activsheet,'Range','N2');
set(ActivsheetRange, 'Value', 'Water bulk Temp. with time(C) ');
ActivsheetRange = get(Activsheet,'Range','N3:N65000');
set(ActivsheetRange, 'Value', T_bulk_w_excel(:));

```

```

ActivsheetRange = get(Activsheet,'Range','D1');
set(ActivsheetRange, 'Value', 'RESULTS FOR Q=0.1g/min,Tw=61.67,Tc=18');

```

```

% Save the workbook
invoke(Workbook, 'SaveAs', 'For Q=0.1g/min');

```

```

total_time = cputime - start_time;
sprintf ('Actual running time of the model %.4f minutes.',(total_time/60) )

```

Appendix C

Properties used in the model (Sample calculation):

Volume fraction of Copper = 0.78;

Volume fraction of Cyanate ester = 1 - Volume fraction of Copper = 1 – 0.78 = 0.22;

Density of Cyanate Ester ($\rho_{cyanate}$) = 1300 Kg/m³;

Density of Copper (ρ_{cu}) = 8933 Kg/m³;

Density of Composite = (Volume fraction of Cu * ρ_{cu}) + (Volume fraction of Cyanate ester * $\rho_{cyanate}$) =
(0.78*1300) + (0.22*8933) = 7.2537*10³ Kg/m³;

Specific heat of Cyanate Ester ($Cp_{cyanate}$) = 865 J / kg-K;

Specific heat of Copper (Cp_{copper}) = 385 J/Kg-K;

Specific heat of Composite = (Volume fraction of Cu * Cp_{copper}) + (Volume fraction of Cyanate ester *
 $Cp_{cyanate}$) = (0.78*385) + (0.22*865) = 490.6J/Kg-K;

Thermal conductivity of Composite (k_c) = 9.9 W/m-K;

Kinematic Viscosity of water at 60°C:

$$\nu_{water} = \frac{1.083+0.708+0.514}{3} \times 10^{-5} \times 9.2903 \times 10^{-2} = 7.13805 \times 10^{-7} \frac{m^2}{s}$$

Prandtl number of water at 60°C:

$$Pr_{Water} = \frac{7.02 + 4.34 + 3.02}{3} = 4.793$$

Thermal conductivity of water at 60°C:

$$k_{Water} = \frac{0.345+0.363+0.376}{3} \times 1.729577 = 0.62495 \frac{W}{m-K}$$

Kinematic Viscosity of water at 80°C:

$$\nu_{water} = \frac{1.083+0.708+0.514+0.392}{4} \times 10^{-5} \times 9.2903 \times 10^{-2} = 6.263987 \times 10^{-7} \frac{m^2}{s}$$

Prandtl number of water at 80°C:

$$P_{r_{Water}} = \frac{7.02 + 4.34 + 3.02 + 2.22}{4} = 4.15$$

Thermal conductivity of water at 80°C:

$$k_{Water} = \frac{0.345 + 0.363 + 0.376 + 0.386}{4} \times 1.729577 = 0.6356 \frac{W}{m-K}$$

Correlation Coefficient (r):

Correlation, (often measured as a correlation coefficient) is a measure of the strength of the relationship between two variables and it ranges from -1.0 to +1.0 [2]. If r is positive, it means that as one variable gets larger the other gets larger. If r is negative it means that as one gets larger, the other gets smaller (often called an "inverse" correlation).

Correlation coefficient is calculated as follows:

$$r = \frac{N \sum XY - \sum X \sum Y}{\sqrt{[N \sum X^2 - (\sum X)^2][N \sum Y^2 - (\sum Y)^2]}}$$

where, N – Number of time steps;

X = Experimental data points;

Y = Predicted data points;

$\sum XY$ = Sum of the product of X and Y;

$\sum X$ = Sum of all the data points of Experimental data;

$\sum Y$ = Sum of all the data points of Predicted data;

$\sum X^2$ = Sum of the square of all the data points of Experimental data;

$\sum Y^2$ = Sum of the square of all the data points of Predicted data;

VITA

Bhargav Telikicherla Kandala was born on September 25th, 1985 in Kakinada, a natural harbor city in Southern India. He pursued his Bachelor's in Mechanical Engineering at Mannan Institute of Science and Technology, Hyderabad, India which is affiliated to Jawaharlal Nehru Technological University. Upon completion he moved to University of Tennessee, Knoxville, USA (www.utk.edu) in the Fall of 2006 to start a graduate study in Mechanical Engineering. While pursuing his Master's, he worked as a Graduate Research Assistant for Dr. Madhu S. Madhukar at the Magnet Development Lab on the Quasi-Poloidal Stellarator project (<http://web.utk.edu/~qps>), which is jointly carried by the Oak Ridge National Lab researchers and UT engineers. He also worked as a Graduate Research Assistant for Dr. David Joy on developing algorithms for post processing the electron beam spectrum data for JEOL Ltd. Japan. He is planning to start his career as a Mechanical Engineer in a professional engineering firm.